Article:
Poyatos-Moré, M, Jones, GD, Brunt, RL et al. (3 more authors) (2016) Mud-dominated basin margin progradation: processes and implications. Journal of Sedimentary Research, 86 (8). pp. 863-878. ISSN 1527-1404

https://doi.org/10.2110/jsr.2016.57

MUD-DOMINATED BASIN MARGIN PROGRADATION: PROCESSES AND IMPLICATIONS

Miquel Poyatos-Moré[1]*, George D. Jones[2], Rufus L. Brunt[1], David M. Hodgson[3], Richard J. Wild[4] and Stephen S. Flint[1]

[1]Stratigraphy Group, School of Earth, Atmospheric and Environmental Sciences, University of Manchester, Manchester M13 9PL, UK

[2]VNG Norge, Filipstad Brygge 1, 0252 Oslo, Norway

[3]Stratigraphy Group, School of Earth and Environment, University of Leeds, Leeds LS2 9JT, UK

[4]Statoil ASA, Exploration Research, Arkitekt Ebbells veg. 10, Rotvoll, Norway

*email: miquel.poyatos-more@manchester.ac.uk

ABSTRACT: The accretion of coarse-grained material at the shelf-edge rollover has been emphasized in studies of basin margin progradation, despite fine grained sediment (clay and silt) representing a volumetrically more significant component of subaqueous clinothems. The timing and processes of fine-grained sediment transport across the shelf and onto the slope remains an understudied facet of sedimentary basin stratigraphy. Three exhumed basin margin-scale clinothems of the Permian Waterford Formation, in the Karoo Basin, South Africa, offer outcrop examples of margin development through the accretion of mud during flooded shelf conditions. The progradation of wave/storm-influenced sandy shelf topset deposits over a thick mudstone succession and beyond a previously established sand-rich shelf-edge rollover suggests that some periods of basin margin progradation took place exclusively via dilute mud-rich gravity flows. Detailed outcrop and core study of offshore mudstones reveals a high content of organic debris and mica. Individual beds show normal and inverse grading, internal erosion surfaces and moderate to low bioturbation, reflecting relatively stressed conditions in frequently supplied outer shelf to upper slope regions. The estimated low gradient (<0.7º) of the Karoo Basin margin and prevailing wave/storm conditions facilitated prolonged suspension of fluid mud and transport across the shelf and beyond the shelf-edge rollover in sediment gravity flows. This study represents a rare example of mudstone-dominated shelf-edge rollover deposits documented at outcrop and core, and demonstrates how fine-grained sediment accretion can play a significant role in basin margin progradation. Conventional depositional models

do not adequately account for progradation of basin margins in the absence of sand supply, which implies potential risks in the identification of shelf edge rollover positions and application of trajectory analysis in strongly progradational margins.

INTRODUCTION

Mud-rich clinothems are major components of continental shelves and the progradation of mud-dominated deltas has been widely described in modern systems (e.g. Cattaneo et al. 2007; Slingerland et al. 2008). Shelf-edge progradation is commonly associated with the accretion of coarse-grained material (very fine sand and coarser) on and beyond the rollover (zone between the topset and foreset), when sedimentation in topsets is limited by low accommodation and/or high sediment supply (Morton and Suter 1996; Muto and Steel 2002; Steel and Olsen 2002; Steel et al. 2003; Johannessen and Steel 2005; Porębski and Steel 2006; Carvajal and Steel 2009; Carvajal et al. 2009; Covault et al. 2009; Olariu and Steel 2009; Hubbard et al. 2010; Dixon et al. 2012a; 2012b). Typically, the recognition of sand-rich shelf-edge rollovers is used in outcrop and subsurface studies to define basin margin clinothems (e.g. Plink-Björklund and Steel 2002; Mellere et al. 2003; Pyles and Slatt 2007; Uroza and Steel 2008; Dixon et al. 2012a) (Fig. 1). The trajectory of multiple shelf-edge rollovers can be used to infer long-term relative sea-level changes (e.g. Steel and Olsen 2002; Helland-Hansen and Hampson 2009; Henriksen et al. 2009; 2011; Olariu et al. 2012). When trajectory is used in combination with the interpreted dominant shelf-edge process regime (Dixon et al. 2012b), the timing of coarse-grained sediment delivery from shelves to deep basins can be predicted.

Mud-grade sediment is a volumetrically significant proportion of the total sediment transferred by rivers (e.g. Burgess and Hovius 1998), and a major sediment component in modern shelf construction (McCave 1972; Nittrouer et al. 1986; Kineke et al. 1996; Kuehl et al. 1996; Kuehl et al. 1997; Michels et al. 1998; Kineke et al. 2000; Liu et al. 2001; Bentley 2003; Hill et al. 2009). Consequently subaqueous deltas, shelf-edge rollovers, and basin margin clinothems are dominated by thick mud(-stone)-rich packages (e.g. Damuth et al. 1988; Bohacs 1998; Driscoll and Karner 1999; Cattaneo et al. 2007; Liu et al. 2007; Slingerland et al. 2008; Bohacs et al. 2014; Patruno et al. 2015) (Fig. 1), despite the emphasis commonly being on their sand-rich components. In addition, oceanographic studies have documented the existence of high energy prograding mud-rich shelves (Rine and

Ginsburg 1985; Augustinus 1989; Allison and Nittrouer 1998; Allison and Neill 2003; Cattaneo et al. 2003; Rotondo and Bentley 2003; Walsh et al. 2004; Ta et al. 2005).

A re-examination of mud transport processes (Macquaker and Bohacs 2007; McAnally et al. 2007; Schieber et al. 2007; Schieber and Southard 2009; Schieber and Yawar 2009) and the mechanisms responsible for widespread distribution of mud along the shelf (Nemec 1995; Abbott 2000; Traykovski et al. 2000; Parsons et al. 2001; Dalrymple and Cummings 2005; Pattison 2005; Nakajima 2006; Macquaker et al. 2007; Varban and Plint 2008; Ichaso and Dalrymple 2009; Macquaker et al. 2010; Ghadeer and Macquaker 2011; Harazim and McIlroy 2015) have led to a major reappraisal of fine-grained successions in ancient shelves and epicontinental seas (e.g. Soyinka and Slatt 2008; Bhattacharya and MacEachern 2009; Plint et al. 2009; MacKay and Dalrymple 2011; Plint et al. 2012; 2014; Wilson and Schieber 2014). However, there remains a lack of detailed studies across ancient mudstone-rich shelf-edge rollover successions (type 4 clinothems of Steel et al. 2000), and the mechanism and timing for basin margin clinothem progradation under mud-dominated supply regimes are still poorly constrained.

This study of the Permian Waterford Formation, Karoo Basin (South Africa), utilizes an established stratigraphic framework (Wild et al. 2009; Jones et al. 2013; 2015), but focuses specifically on documenting a particular style of mudstone-dominated basin margin progradation in two basin margin-scale clinothems. The combined outcrop and core dataset permits to i) recognize and provide a depositional model of the shelf-to-slope transition in fine grained successions; ii) to understand the processes responsible for the transport and deposition of outer shelf and upper slope mudstones; and iii) to consider and discuss the implications of basin margin growth in the absence of coarse-grained sediment delivery at the shelf edge.

STUDY AREA AND DATASET

The 5500-m-thick Karoo Supergroup in the SW Karoo Basin of South Africa comprises the Dwyka Group (Late Carboniferous to Early Permian glacial deposits), the Ecca Group (Permian clastic marine/marginal marine) and the Beaufort Group (Permo–Triassic fluvial sediments) (Veevers et al. 1994; Johnson et al. 1997; Visser 1997; Rubidge et al. 2000; Cole and Whipplinger 2001) (Fig. 2). Subsidence during Ecca Group time was generated by a combination of dynamic topography related to subduction of the paleo-Pacific oceanic plate, and inherited basement structures (Visser and

Praekelt 1996; Pysklywec and Mitrovica 1999; Tankard et al. 2009), that led to the development of the Tanqua and Laingsburg depocenters.

The Karoo Basin deep water succession (Wickens 1994; Hodgson et al. 2006; Flint et al. 2011) is overlain by upper slope and shelf deposits of the Waterford Formation (Wickens 1994) (Fig. 2), a 400 m-thick mixed-influence deltaic succession (Wild et al. 2009; Oliveira et al. 2011; Jones et al. 2013). The complete vertical stratigraphic transition from slope channel-levee systems (Wild et al. 2005; Hodgson et al. 2011) to shelf deltas, in combination with extensive down-dip exposures, permits the geometry of the basin margin to be reconstructed, and the identification of successive basin margin clinothems and their shelf-edge rollover positions (Wild et al. 2009; Oliveira et al. 2011; Dixon et al. 2012a; Jones et al. 2013; 2015). Recent improved constraints on the timing of sedimentation from U-Pb volcanic ash dating (Fildani et al. 2007; Fildani et al. 2009; McKay et al. 2015) suggest deltaic deposition began slightly earlier in the Tanqua than in the Laingsburg depocenter. However, the correlation of time-equivalent units between both depocenters is not the objective of this paper.

The dataset in the 6000 km^2 study area (Fig. 2) includes 66 detailed logged sections (15 in Tanqua, 51 in Laingsburg) and a 550 m fully cored research borehole (SL1), that collectively total nearly 21 km of measured thickness, with units walked out between logs to provide physical stratigraphic correlation. The outcrop dataset from both depocenters is displayed in >40 km-long correlation panels (Figs. 3, 4). Collection of unidirectional paleoflow measurements from ripple foresets and flute casts, and bidirectional measurements from groove marks and the crest-lines of symmetrical ripples indicate that the overall paleoflow was to the NE and E (030°-080°) such that the panels are sub-parallel to depositional dip, with landward to the west and south and basinward to the east and north. Panels in Laingsburg are about 6 km apart across depositional strike, providing three-dimensional control on sedimentological characteristics and depositional architecture for each clinothem (Jones et al. 2015).

FACIES ANALYSIS

The sedimentary facies scheme is largely based on previous studies (Wild et al. 2009; Oliveira et al. 2011; Jones et al. 2013) and is presented in Table 1. The sand-dominated facies associations of the Waterford Formation topset deposits exhibit characteristics that are consistent with mixed wave- and river-influenced shoreline settings (Reineck and Singh 1973; Harms et al. 1975; 1982; McCubbin 1982; Browning et al. 2006; Ainsworth et al. 2011). This work focusses on the range of facies and

facies associations that span from outer shelf through shelf-edge rollover to upper slope depositional settings (Table 1). Overall, the amount of Sedimentary structures that indicate river-dominance is less in Laingsburg than in Tanqua, and therefore shoreface nomenclature is used to interpreted the depositional environments in the Laingsburg area (Jones et al. 2013; 2015), but a delta-front/shoreface nomenclature is maintained for the Tanqua area (Wild et al. 2009).

CLINOTHEMS – UNITS OF BASIN MARGIN PROGRADATION

The stratigraphic units of the lower Waterford Formation are interpreted as basin margin clinothems, the fundamental building blocks of basin margin development (e.g. Steel and Olsen 2002; Helland-Hansen et al. 2012; Patruno et al. 2015) (Fig. 1). Wild et al. (2009) and Jones et al. (2013) recognized multiple 10-100 m-thick clinothems along depositional dip profiles (Figs. 3, 4), in Tanqua and Laingsburg respectively. The vertical profile, depositional setting and scale of these stratigraphic packages are consistent with deltaic parasequences as described by Van Wagoner et al. (1990). Constraining the complete topset, foreset and bottomset deposits for each individual clinothem is not always possible. However, the basinward thickening of parasequences, defined by regional mudstone units interpreted to contain the deepwater equivalent of flooding surfaces, can be recognized and used to define clinothems (Dixon et al. 2012b; Jones et al. 2015). The first abrupt or significant change in the gradient can be used to interpret the location of successive shelf edge rollovers (Southard and Stanley 1976), but the ‘apparent’ geometry of ancient shelf margins might be highly dependent on the choice of datum and the result of post-depositional factors, such as differential sand/mud compaction and accumulated error when measuring thicknesses in the field. This geometric criterion must be therefore used in combination with other observed features, which do not independently point the shelf edge position, but that in conjunction indicate abrupt changes in sedimentary facies and depositional architecture close to the shelf-edge rollover zone. These include (i) extensional deformation (growth faults), (ii) widespread bypass features (gullies) and (iii) progressive increase in sandstone turbidites beyond the rollover (see Jones et al. 2013).

In the up-dip exposures, clinothem thickness decreases stratigraphically upward from ~50 m to ~25 m in Tanqua, and from ~100 m to ~20 m in Laingsburg (Table 2). The documented NE and E paleoflow direction in both the Tanqua and Laingsburg depocenters is consistent with a NW-SE orientation of

149 the reconstructed shelf margin, although with local irregularities and lateral variability as reported in
150 the Laingsburg depocenter (Jones et al. 2015) (Fig. 5).
151
152 **STRATIGRAPHIC ARCHITECTURE**
153 *Laingsburg depocenter*
154 The lower Waterford Formation in the Laingsburg area comprises eight regionally-correlated
155 clinothems (Jones et al. 2015). The lower four units (WfC-1-4) show a progradational stacking pattern
156 interpreted as a highstand systems tract (Jones et al., 2013). WfC 4 and 5 are separated by an
157 interpreted regressive surface of marine erosion (type-2 sequence boundary, Fig. 4) (Jones et al.
158 2013). Clinothems show an increasingly steep rising trajectory with the shelf-edge rollover of WfC 5
159 positioned almost directly on top of the rollover of WfC 4 (Fig. 4) (Jones et al. 2015). WfC 5
160 represents the final sand-dominated shoreface system established at the shelf-edge rollover, and with
161 an overlying 5-10 m-thick basinward thickening mudstone is interpreted as a transgressive systems
162 tract (TST) and associated maximum flooding surface (MFS) that marks the retreat of the system to
163 an inner shelf position (Fig. 4). WfC 6 and 7 consist primarily of heterolithic shoreface/offshore
164 transition (SOT) deposits with poorly developed amalgamated lower shoreface facies only observable
165 in their proximal exposures (Figs. 5, 6, 7). The seaward pinchout of the sand-rich shoreface facies of
166 WfC 6 is 10-15 km updip from the shelf-edge rollover position of WfC 5, and the shoreface component
167 of WfC 7 is progradational relative to WfC 6 but also fines and pinches out to a minimum of 5 km
168 landward of the shelf-edge rollover of WfC 5 (Figs. 5, 7). The basinward stepping of WfC 6 and 7
169 suggests that the system returned to a progradational trend as part of the subsequent highstand
170 systems tract. However, the lack of coarse-grained material in WfC 6 and 7 beyond the shelf-edge
171 rollover position of WfC 5 in some areas along the shelf margin (Figs. 5) indicates that the sand-rich
172 components of WfC 6 and 7 remained on the inner shelf (shelf-confined; Fig. 1). Correlations along
173 the Zoutkloof area show that sand-rich shoreface facies associations of WfC 8 extend for 15 km
174 beyond the last sand-defined shelf edge of WfC 5 (Jones et al. 2015) and well beyond the inner shelf
175 sand-rich pinch-outs of WfC 6 and 7 (Fig. 7). Therefore, during WfC 6, 7 and lower WfC 8 the shelf-
176 edge rollover prograded ~15 km (distance from the lower sand-rich rollover position identified in WfC
177 5 to the sand-rich shelf-edge rollover of WfC 8) through the accretion of mud under sea level
178 highstand conditions.

179

180 *Tanqua depocenter*

181 The stratigraphic architecture of the lower Waterford Formation clinothems (C1-C8, Fig. 3) in the
182 Tanqua depocenter is similar to that described in Laingsburg but the correlation between both
183 successions is not established due to the lack of absolute age control. Differences (Table 2) include
184 thinner clinothems combined with lower estimated gradients (0.5° to 0.7°, using compacted
185 thicknesses) (see also Wild et al. 2009), and a thinner underlying channelized slope succession (Wild
186 et al. 2005; Hodgson et al. 2006), suggesting a lower-gradient margin and a shallower basin margin
187 relief in the Tanqua depocenter.

188 Clinothems C2–4 exhibit a strongly aggradational to progradational stacking pattern and rising
189 shoreline and shelf edge rollover trajectory, interpreted as part of a highstand systems tract (Wild et
190 al. 2009), culminating in the maximum regression point in C4-5, with the rollover located close to the
191 SL1 locality (Fig. 3). The sandstone pinch-out of the overlying clinothem C5 is positioned slightly
192 landward of the sand-rich rollover of C4, south of SL1-Bitterberg (T5), suggesting a turnaround to a
193 retrogradational stacking pattern. This, together with an overlying regionally extensive mudstone is
194 interpreted to be part of a transgressive systems tract (TST) and early HST, and contain an
195 associated MFS, at which time the shoreline stepped back onto a more landward shelf position (Fig.
196 3).

197 Clinothem C6 consists of amalgamated organic-rich delta front/shoreface facies associations (Table
198 1) that are only recognized in the most proximal exposures (T2-T3, Fig. 3). The sand-rich component
199 of C6 fines and thins basinward, and pinches out between Vaalberg and Bitterberg (T4 and T5, Fig.
200 3), i.e., before the established shelf-edge rollover position of C5. Clinothem C7 prograded over C6
201 and its delta front/shoreface sandstones pinchout beyond the previous shelf-edge rollover position of
202 C5, reaching the westernmost edge of the study area in Katjiesberg (T7, Fig. 3). The progradational
203 stacking pattern of C6 and C7 is consistent with the lower part of a second highstand systems tract
204 after the regional transgressive event in C5. The absence of sand-rich C6 deposits basinward of the
205 rollover position of C5 is consistent with deltaic/shoreface sandstones confined in the inner shelf and
206 with a mudstone-dominated shelf edge and upper slope. Sand-rich facies associations in C7 can be
207 followed basinward for 10 km beyond the sand-rich rollover positions of C4 and C5 and well beyond

208 the sandstone pinch out of C6 (Fig. 3). This indicates that during C6 and early C7 time, the shelf-edge
209 rollover also prograded through the accretion of mud under sea level highstand conditions.
210
211 **MUDSTONE-DOMINATED SHELF EDGE DEPOSITS**
212 *Outcrop observations*
213 WfC 6 and 7 are well exposed in the Zoutkloof area of the Laingsburg depocenter (Fig. 6, see location
214 in Fig. 4A). Detailed outcrop observations just above shoreface-offshore transition (SOT, Table 1)
215 deposits of WfC 5 reveal an 8 m-thick fining-upward package overlain by a 33 m-thick coarsening-
216 and thickening-upward package (Fig. 6). The lower package starts with highly bioturbated coarse
217 siltstones, showing a distinctive mottled texture with an irregular distribution of sand grains within a
218 silty matrix. Overlying these siltstones are multiple surfaces with associated iron-rich nodular
219 horizons, interpreted to record condensed sections and are therefore included in the upper part of the
220 TST associated with WfC 5 (Figs. 6, 7, Table 1). Just above the best developed of these surfaces,
221 considered to be recording the maximum flooding surface, facies pass abruptly into darker, finer-
222 grained and laminated siltstones, rich in organics and mica. These thin beds feature mm-scale
223 dominantly unidirectional to combined-flow tractional structures with little to no bioturbation,
224 interpreted as the oldest most distal deposits of WfC 6 (Fig. 6). Thin beds alternate with diffusely
225 bedded structureless fine siltstones, and become progressively coarser and cleaner up section, losing
226 their organic content while retaining a low to moderate bioturbation index. An overlying pervasively
227 bioturbated 1.2 m-thick package is interpreted to record the transgressive top of WfC 6. The overlying
228 WfC 7 succession coarsens- and thickens-upward from sandstones with symmetrically rippled tops to
229 thicker-bedded sandstones with hummocky cross-stratification (Table 1). The stacking pattern and
230 facies characteristics of WfC 6 and 7 are consistent with an upward transition from offshore/distal
231 prodelta mudstones deposited initially below storm wave base to progressively sandier and shallower
232 wave-influenced deposits (Fig. 6, Table 1). The soft-sediment deformation features observed in WfC 7
233 are interpreted to record delta front/shoreface collapse (Oliveira et al. 2011) (Fig. 7, Table 1). WfC 8
234 starts with moderately-bioturbated and laminated prodeltaic thin beds, but records a more abrupt
235 transition into sand-rich shoreface facies associations (Fig. 6).
236
237 *Core observations*

238 Core observations of the SL1 research borehole (Wild et al. 2009) drilled close to the Bitterberg
239 locality (T5, Figs. 3, 8) of the Tanqua depocenter allowed subtle variations in the characteristics of
240 fine-grained deposits in the C6-C7 succession to be documented (Fig. 8). The stratigraphic control
241 indicates that in the core, this mudstone-dominated package overlies the maximum flooding surface
242 above C5, and captures deposition across the shelf-edge rollover (Fig. 3). Analysis included detailed
243 (mm-scale) logging of the whole 40 m-thick C6-C7 package, with special attention to the stacking
244 pattern and sedimentological features of thin beds to allow an accurate description and interpretation
245 of processes (Fig. 8).
246 Observations reveal the presence of mm to cm-scale organic and mica-rich laminated siltstone layers,
247 interbedded with few bioturbated and/or structureless mudstones (Fig. 8). Parallel- and ripple-
248 laminated siltstones show normal and/or inverse grading, and a range of internal erosion and traction
249 structures within a single bed, along with small-scale soft-sediment deformation (Fig. 8) towards the
250 basal contact of the beds. Sedimentary structures, when observed, mostly include undulate bedding,
251 starved current ripples and apparent planar lamination (Schieber et al. 2010). Some beds show a
252 distinctive two-part organization with a clean, laminated silt-rich lower part, preserving primary
253 structures and an erosive and/or loaded base (Fig. 8), overlain with a sharp contact by a finer and
254 darker poorly sorted/bioturbated upper section, rich in mud clasts and containing mica and plant
255 debris (Fig. 9). Bioturbation intensity generally ranges from moderate to low (Bioturbation Index 0-2)
256 (e.g. Taylor et al. 2003). Evidence of combined-flow indicators can be inferred from low
257 angle/undulated cross laminations in the coarser beds of these fine-grained intervals (Fig. 8).
258
259 *Characterization of mudstones at the shelf-edge rollover*
260 The outcrop examples of Laingsburg WfC 6 and 7 in the Zoutkloof panel (Fig. 7) combined with the
261 core observations of Tanqua C6 and C7 in the SL1 well (Fig. 8), offer the opportunity to study two
262 unusual examples of fine-grained shelf to slope transitions. These mudstone thin beds are grouped
263 according to their interpreted sedimentary processes and inferred position along the depositional
264 profile (*Types A-D*; Fig. 10).
265 *Type-A* beds are mainly composed of coarse siltstone with sharp base and top, and combined- to
266 unidirectional-flow tractional structures. *Type-A* beds dominate the upper (and more proximal) parts of
267 mudstone-dominated clinothems in WfC 6-7 in Zoutkloof (Fig. 6) and in C6-7 in the SL1 well (Fig. 8),

and are also commonly seen interbedded with wave-dominated sand-rich thin beds in shoreface-offshore transition deposits (Fig. 6, Table 1). These beds (0.5-2 cm-thick) are interpreted to record the most proximal expression of dilute silt-rich gravity-flows in distal prodelta/outer shelf settings, sometimes under the effect of storm/waves (undulate cross laminations observed might be the product of storm reworking), and with the sharp bed tops indicative of basinward bypass (Stevenson et al. 2015) of finer particles (Fig. 10).

Type-B beds have sharp, erosive/loaded bases with a distinctive bipartite character that comprises a lower (0.5-2 cm-thick) well-sorted silt-rich, parallel to low angle laminated part, overlain by a mud/organic-rich poorly-sorted upper section (1-2 cm-thick; Fig. 10). The poorly sorted part commonly drapes a scour surface (Fig. 9,). *Type-B* beds are interpreted to record a longitudinal change in flow properties within the same event, associated with flow acceleration due to sediment entrainment and/or gradient increase at the shelf edge. This flow transformation is recorded in the sharp intra-bed facies change from the clean and well-sorted laminated basal part to the poorly sorted argillaceous part overlying an erosion surface. The basal part is interpreted as the deposit of a waxing underflow, and the upper part as a muddy debrite, with the erosion surface between suggesting a phase of basinward sediment bypass. *Type-B* beds dominate intermediate sections of the studied intervals (Fig. 8).

Type-C beds form 2-4 cm-thick inverse-graded beds with a gradational base, relatively sharp, mudstone clast-rich tops sometimes overlain by a finer and moderately bioturbated normally graded upper part, and a general absence of bioturbation (Fig. 8). Their character suggests an accelerating/waxing flow origin and entrainment of seafloor material and/or lofted mud-size particles from the turbid ambient fluid (Fig. 10). The sharp tops suggest basinward sediment bypass. *Type-C beds* are less common than other bed types, and occur in the lower parts of the studied sections, suggesting deposition occurred where gradient progressively increased towards the upper slope (Fig. 10).

Type-D beds are generally 0.5-7 cm-thick, sharp-based and normally graded with traction structures and grade into well-developed mud-rich tops with moderate bioturbation (B.I. 2) and abundant organic debris and mica. They are interpreted to record deposition of the dilute part of a waning sediment gravity flow across the shelf-to-slope transition (Fig. 10). Although *Type-D beds* are found throughout the entire succession, they are more common in the lower part of the studied sections (Fig. 8),

suggesting they record deposition in a more distal setting under relatively quieter conditions. Locally, *Type-C* and *Type-D beds* combine to form inverse- to normally-graded beds, which has been used as diagnostic criteria for deposition from hyperpycnal flows (Mulder et al. 2003; Plink-Björklund and Steel 2004; Zavala et al. 2007).

DISCUSSION

Implications for basin margin analysis

Large-scale correlation within the lower Waterford Formation demonstrates that some periods of basin margin progradation were exclusively through the accretion of mud (clay and silt) across the shelf-edge rollover and onto the upper slope. In the Laingsburg depocenter, during WfC 6 and 7 and early WfC 8, shelf margin accretion and progradation took place in the absence of coarse-grained sediment supply under flooded shelf conditions. Sufficient accommodation and shallow water depths led to the development of low-amplitude (5-30 m-thick) mud-rich and shelf-confined delta clinothems (Figs. 1, 6). However, at this time the shelf-edge rollover prograded a minimum of 15 kilometers via deposition of mud-rich flows, down dip from time equivalent shelf-confined sand-rich delta fronts/shorefaces (Figs. 6, 10). During periods of high relative sea level, although the sand-rich component of deltas mostly accumulates on the inner shelf (e.g. Porębski and Steel 2006), the shelf edge is still present as a physiographic feature, but is muddier and more attenuated (Olariu and Steel 2009). In the absence of absolute age control in the Karoo Basin the rates of aggradation and progradation cannot be constrained. These results contrast with 'classic' seismic sequence stratigraphy, that was developed to understand and predict the spatial and temporal distribution of potential reservoir sand bodies in relation to accommodation history of basin margins (Vail et al. 1977; Posamentier et al. 1988; Posamentier and Vail 1988; Van Wagoner et al. 1990). Therefore, depositional models have paid little attention to the large volume and processes of fine-grained sediment delivery to build the shelf prism, and instead emphasize the timing of sand transfer to the slope and basin floor, as a response to relative sea level change (e.g. Helland-Hansen and Hampson 2009). During periods of low relative sea level, the shelf margin position tends to move basinward, but part or all of the shelf may become exposed subaerially, and the shelf and shelf-edge rollover areas will be subject to sediment bypass and local degradation (Ross et al. 1994; Hadler-Jacobsen et al. 2005; Ryan et al. 2009).

328

329 *Muddy shelf-edge rollovers and clinoform trajectories*

330 Most studies of ancient clinothems and shelf margins focus on the process regime and architecture of
331 sand-rich deposits to support shelf-edge rollover identification (e.g. Plink-Björklund and Steel 2002;
332 Mellere et al. 2003; Pyles and Slatt 2007; Uroza and Steel 2008; Hubbard et al. 2010; Dixon et al.
333 2012a; Jones et al. 2013). The present study demonstrates that shelf-edge rollovers are not always
334 defined by sand-rich deposits, yet can still be identified at outcrop based on geometry and detailed
335 sedimentology. Under flooded shelf conditions, the mud-rich extended bottomset component of
336 deltaic clinothems may reach the upper slope, to build fine-grained shelf-edge rollovers and basin
337 margin clinothem foresets that prograde basinward. This occurs when the sand-rich topset and
338 foreset component of delta-scale clinothems is confined to the inner part of the shelf (Fig. 1). Analysis
339 of the lower Waterford Formation clinothems highlights a potential limitation of shelf-edge trajectory
340 analysis; delivery systems are observed to change laterally from shelf-confined to shelf-edge (e.g.
341 Sanchez et al. 2012; Jones et al. 2015) (Figs. 1, 11), however the clinothem trajectory may remain
342 consistently progradational. An example of this can be found in the Upper Cretaceous Fox Hills
343 Formation (Wyoming, USA), where, although most of prograding clinothems are dominated by sand,
344 some examples have shelf edge rollovers dominated by mud (clinothems C06, C07 and C12, Olariu
345 et al. 2012). The expression of shelf-edge rollovers and parasequence boundaries of muddy
346 clinothems are challenging to identify, and the time they represent is difficult to constrain (Bohacs
347 1998). This is particularly true in subsurface studies, due to the complex recognition of impedance
348 contrasts (Miller et al. 2013). As in the Waterford Formation, under relative sea level highstand
349 conditions, the delta top sand-rich components of some parasequences can be confined in inner shelf
350 positions, remaining below seismic resolution, but the shelf margin can still prograde through the
351 accretion of mud (Fig. 11). The position of highstand deposits relative to the shelf margin can be
352 problematic in exploration studies, because muddy parasequences may have laterally extensive,
353 comparatively sand-dominated topsets (Figs. 5, 11) and therefore require the presence of regional,
354 transgressive mudstones to develop effective seals.

355

356 *Sediment transport on a high-energy muddy shelf*

357 The integration of outcrop data with detailed core analysis shows that mud-dominated shelf margin
358 progradation was the result of deposition of muddy and organic-rich sediment gravity flows. The
359 significant amount of plant debris and mica in some beds indicates a continental origin of mud,
360 possibly from hyperpycnal river plumes (Mulder and Alexander 2001; Mulder et al. 2003; Bouma and
361 Scott 2004; Plink-Björklund and Steel 2004; Zavala et al. 2006a; 2006b; Bhattacharya and
362 MacEachern 2009; Zavala et al. 2012). However, the common occurrence of wave/storm processes
363 that influenced the deposition of sand-rich deposits in shoreface and shoreface-offshore transition
364 settings (Table 1) (Jones et al. 2015), combined with a relatively low gradient (Table 2), is not
365 consistent with the characteristics of margins where fine-grained sedimentation is associated with
366 recurrent and sustained hyperpycnal discharges to the shelf edge (Mutti et al. 1996; Bentley 2003;
367 Mulder et al. 2003; Mutti et al. 2003; Plink-Björklund and Steel 2004; Friedrichs and Scully 2007).
368 Wave/storm processes are therefore advocated to be the main mechanism that kept unconsolidated
369 silt and flocculated clay fraction in suspension, or re-suspended (e.g. Traykovski et al. 2000; Pattison
370 2008; Macquaker et al. 2010). Mud particles that accumulate as floccules or organo-mineralic
371 aggregates (Plint 2014) act hydrodynamically as silt or sand grains (Schieber et al. 2007). This is
372 supported by the ubiquity of tractional structures observed within the thin mudstone beds. Wave
373 enhancement of gravity flows or storm re-suspension of previously-deposited sediment can occur
374 before, during, or shortly after river flood events (Ogston et al. 2000; Traykovski et al. 2000; Fan et al.
375 2004), but the process is more commonly identified in systems that are not able to deliver significant
376 amounts of new mud to the shelf (Bentley et al. 2006). The paucity of combined-flow indicators in bed
377 *Types B to D* (Fig. 10) contrasts with their presence in *Type A beds* and their presence in the
378 shoreface and shoreface-offshore transition sandy counterparts (Fig. 6 and Table 1). This is
379 interpreted to indicate that, although waves/storms played an important role keeping mud in
380 suspension across the shelf, deposition of the finest particles in the studied sections took place mostly
381 below storm wave base as sediment gravity flows (e.g. Pattison 2005). Erosive and sharp boundaries
382 within beds, and internal scours draped by poorly-sorted mudstones suggest sediment bypass and
383 downslope transformation from waxing to waning gravity-driven flows. This, together with the low
384 bioturbation intensity and diversity within the thin, silty beds, reflects environmental stresses and high
385 sedimentation rates in outer shelf to upper slope settings of mud-dominated clinoforms.
386

CONCLUSIONS

Three parasequences from exhumed and well-constrained basin margin clinothems of the Permian Waterford Formation, in adjacent depocenters of the Karoo Basin (South Africa), provide the first examples of mudstone-dominated shelf-edge rollover deposits documented in outcrop and core. This dataset has allowed the timing and processes of fine-grained sediment transport across the shelf and onto the slope to be assessed. The study demonstrates that some periods of shelf-edge progradation occurred through the accretion of mud when the sand-rich part of wave-influenced deltas was positioned on the inner shelf. Detailed analysis of offshore mudstones suggests that recurrent supply to outer shelf and upper slope regions was by micaceous and organic-rich fluid mud that was kept in suspension or re-suspended from inner shelf positions during storms and transported across the low gradient shelf as dilute silt-rich gravity flows. Thin bed characteristics at the shelf-edge rollover and upper slope include soft-sediment deformation, evidence of sediment bypass including sharp contacts, internal erosions and traction structures and a subtle downdip facies changes within low density, silty turbidites. This work demonstrates that processes responsible for the transport and deposition of fine-grained material across and beyond the shelf edge play a fundamental role in basin margin development. The documentation of mud-rich shelf to slope transitions is significant for outcrop and subsurface investigations, because clinothems are not always defined by sand-rich shelf-edge rollovers, and significant basin margin progradation can also occur in the absence of coarse-grained sediment supply. This implies potential risks in the identification of shelf-edge rollover positions from presence of sand alone, and in the use of trajectory analysis to interpret relative sea-level changes and to predict down dip sand supply.

ACKNOWLEDGEMENTS

The authors thank the Slope project Phase 4 sponsors for financial support: Anadarko, BHP Billiton, BP, ConocoPhillips, E-ON, Engie, Maersk, Murphy, Nexen-CNOOC, Petrobras, Shell, Statoil, Total, VNG Norge and Woodside. De Ville Wickens is acknowledged for his logistical support and insightful discussions in the field. Landowners are thanked for permission to their land. Luz Gomis, Colleen Kurcinka, Daniel Bell, Lewis Burden, Eoin Dunlevy and Xavier Solé are thanked for their assistance. This manuscript has benefited from the insightful comments and reviews of Andrea Fildani, Cornel Olariu, Guy Plint and Carlo Messina.

417

418

REFERENCES

ABBOTT, S.T., 2000, Detached mud prism origin of highstand systems tracts from mid-Pleistocene sequences, Wanganui Basin, New Zealand: Sedimentology, v. 47, p. 15-29.

AINSWORTH, R.B., VAKARELOV, B.K., and NANSON, R.A., 2011, Dynamic spatial and temporal prediction of changes in depositional processes on clastic shorelines: Toward improved subsurface uncertainty reduction and management: AAPG Bulletin, v. 95, p. 267-297.

ALLISON, M.A., and NEILL, C.F., 2003, Development of a modern subaqueous mud delta on the Atchafalaya Shelf, Louisiana, *in* Scott, E.D., Bouma, A.H., and Bryant, W.R., eds., Siltstones, Mudstones and Shales: Depositional Processes and Characteristics: SEPM, CD-ROM, p. 23-34.

ALLISON, M.A., and NITTROUER, C.A., 1998, Identifying accretionary mud shorefaces in the geologic record: insights from the modern Amazon dispersal system, *in* Schieber, J., Zimmerle, W., and S. Sethi, P., eds., Shales and mudstones: Recent Progress in Shale Research: Stuttgart, Schweizerbart'sche Verlagsbuchhandlung, Stuttgart, Germany, p. 147-161.

AUGUSTINUS, P.G.E.F., 1989, Cheniers and chenier plains: a general introduction: Marine Geology, v. 90, p. 219-229.

BENTLEY, S.J., 2003, Wave-current dispersal of fine-grained fluvial sediments across continental shelves: the significance of hyperpycnal plumes, *in* Scott, E.D., Bouma, A.H., and Bryant, W.R., eds., Siltstones, Mudstones and Shales: Depositional Processes and Characteristics: SEPM, CD-ROM, p. 35-48.

BENTLEY, S.J., SHEREMET, A., and JAEGER, J.M., 2006, Event sedimentation, bioturbation and preserved sedimentary fabric: field and model comparisons in three contrasting marine settings: Continental Shelf Research, v. 26, p. 2108-2124.

BHATTACHARYA, J.P., and MACEACHERN, J.A., 2009, Hyperpycnal rivers and prodeltaic shelves in the Cretaceous seaway of North America: Journal of Sedimentary Research, v. 79, p. 184-209.

BOHACS, K.M., 1998, Contrasting expressions of depositional sequences in mudrocks from marine to non marine environs, *in* Schieber, J., Zimmerle, W., and Sethi, P.S., eds., Shales and mudstones: Recent Progress in Shale Research: Schweizerbart'sche Verlagsbuchhandlung, Stuttgart, Germany, p. 33–78.

449 BOHACS, K.M., LAZAR, O.R., and DEMKO, T.M., 2014, Parasequence types in shelfal mudstone strata—
450 Quantitative observations of lithofacies and stacking patterns, and conceptual link to modern
451 depositional regimes: Geology, v. 42, p. 131-134.
452 BOUMA, A.H., and SCOTT, E.D., 2004, A review of knowledge about fine-grained sediments:
453 mudstones, siltstones and shales, *in* Scott, E.D., and Bouma, A.H., eds., Depositional
454 Processes and Reservoir Characteristics of Siltstones, Mudstones and Shales, Volume 2:
455 SEPM, CD-ROM, p. 9-23.
456 BROWNING, J.V., MILLER, K.G., MCLAUGHLIN, P.P., KOMINZ, M.A., SUGARMAN, P.J., MONTEVERDE, D.,
457 FEIGENSON, M.D., and HERNÁNDEZ, J.C., 2006, Quantification of the effects of eustasy,
458 subsidence, and sediment supply on Miocene sequences, mid-Atlantic margin of the United
459 States: Geological Society of America Bulletin, v. 118, p. 567-588.
460 BURGESS, P.M., and HOVIUS, N., 1998, Rates of delta progradation during highstands: consequences
461 for timing of deposition in deep-marine systems: Journal of the Geological Society, v. 155, p.
462 217-222.
463 CARVAJAL, C., and STEEL, R., 2009, Shelf-edge architecture and bypass of sand to deep water:
464 influence of shelf-edge processes, sea level, and sediment supply: Journal of Sedimentary
465 Research, v. 79, p. 652-672.
466 CARVAJAL, C., STEEL, R., and PETTER, A., 2009, Sediment supply: The main driver of shelf-margin
467 growth: Earth-Science Reviews, v. 96, p. 221-248.
468 CATTANEO, A., CORREGGIARI, A., LANGONE, L., and TRINCARDI, F., 2003, The late-Holocene Gargano
469 subaqueous delta, Adriatic shelf: sediment pathways and supply fluctuations: Marine
470 Geology, v. 193, p. 61-91.
471 CATTANEO, A., TRINCARDI, F., ASIOLI, A., and CORREGGIARI, A., 2007, The Western Adriatic shelf
472 clinoform: energy-limited bottomset: Continental Shelf Research, v. 27, p. 506-525.
473 COLE, D.I., and WHIPPLINGER, P.E., 2001, Sedimentology and molybdenum potential Beaufort Group
474 in the Karoo Basin: Council for Geoscience, Geological Survey of South Africa. Memoir 80.
475 COVAULT, J.A., ROMANS, B.W., and GRAHAM, S.A., 2009, Outcrop Expression of a Continental-Margin-
476 Scale Shelf-Edge Delta from the Cretaceous Magallanes Basin, Chile: Journal of
477 Sedimentary Research, v. 79, p. 523-539.

478 DALRYMPLE, R.W., and CUMMINGS, D.I., 2005, The offshore transport of mud: why it doesn't happen
479 and the stratigraphic implications: Geological Society of America Abstracts with Programs, v.
480 37, p. 403.
481 DAMUTH, J.E., FLOOD, R.D., KOWSMANN, R.O., BELDERSON, R.H., and GORINI, M.A., 1988, Anatomy
482 and growth pattern of Amazon deep-sea fan as revealed by long-range side-scan sonar
483 (GLORIA) and high resolution seismic studies.: AAPG Bulletin, v. 72, p. 885-911.
484 DIXON, J.F., STEEL, R.J., and OLARIU, C., 2012a, River-dominated, shelf-edge deltas: delivery of sand
485 across the shelf break in the absence of slope incision: Sedimentology, v. 59, p. 1133-1157.
486 DIXON, J.F., STEEL, R.J., and OLARIU, C., 2012b, Shelf-edge delta regime as a predictor of deep-water
487 deposition: Journal of Sedimentary Research, v. 82, p. 681-687.
488 DRISCOLL, N.W., and KARNER, G.D., 1999, Three-dimensional quantitative modeling of clinoform
489 development: Marine Geology, v. 154, p. 383-398.
490 FAN, S., SWIFT, D.J.P., TRAYKOVSKI, P., BENTLEY, S., BORGELD, J.C., REED, C.W., and NIEDORODA,
491 A.W., 2004, River flooding, storm resuspension, and event stratigraphy on the northern
492 California shelf: observations compared with simulations: Marine Geology, v. 210, p. 17-41.
493 FILDANI, A., DRINKWATER, N.J., WEISLOGEL, A., MCHARGUE, T., HODGSON, D.M., and FLINT, S.S., 2007,
494 Age Controls on the Tanqua and Laingsburg Deep-Water Systems: New Insights on the
495 Evolution and Sedimentary Fill of the Karoo Basin, South Africa: Journal of Sedimentary
496 Research, v. 77, p. 901-908.
497 FILDANI, A., WEISLOGEL, A., DRINKWATER, N.J., MCHARGUE, T., TANKARD, A., WOODEN, J., HODGSON, D.,
498 and FLINT, S., 2009, U-Pb zircon ages from the southwestern Karoo Basin, South Africa—
499 Implications for the Permian-Triassic boundary: Geology, v. 37, p. 719-722.
500 FLINT, S.S., HODGSON, D.M., SPRAGUE, A.R., BRUNT, R.L., VAN DER MERWE, W.C., FIGUEIREDO, J.,
501 PRÉLAT, A., BOX, D., DI CELMA, C., and KAVANAGH, J.P., 2011, Depositional architecture and
502 sequence stratigraphy of the Karoo basin floor to shelf edge succession, Laingsburg
503 depocentre, South Africa: Marine and Petroleum Geology, v. 28, p. 658-674.
504 FRIEDRICHS, C.T., and SCULLY, M.E., 2007, Modeling deposition by wave-supported gravity flows on
505 the Po River prodelta: from seasonal floods to prograding clinoforms: Continental Shelf
506 Research, v. 27, p. 322-337.

507 GHADEER, S.G., and MACQUAKER, J.H., 2011, Sediment transport processes in an ancient mud-
508 dominated succession: a comparison of processes operating in marine offshore settings and
509 anoxic basinal environments: Journal of the Geological Society, v. 168, p. 1121-1132.
510 HADLER-JACOBSEN, F., JOHANNESSEN, E.P., ASHTON, N., HENRIKSEN, S., JOHNSON, S.D., and
511 KRISTENSEN, J.B., 2005, Submarine fan morphology and lithology distribution: a predictable
512 function of sediment delivery, gross shelf-to-basin relief, slope gradient and basin
513 relief/topography: Petroleum Geology: North West Europe and Global Perspectives,
514 Proceedings of the 6th Petroleum Geology Conference, London (UK), p. 1121-1145.
515 HARAZIM, D., and MCILROY, D., 2015, Mud-Rich Density-Driven Flows Along an Early Ordovician
516 Storm-Dominated Shoreline: Implications for Shallow-Marine Facies Models: Journal of
517 Sedimentary Research, v. 85, p. 509-528.
518 HARMS, J.C., SOUTHARD, J.B., SPEARING, D.R., and WALKER, R.G., 1975, Depositional environments
519 as interpreted from primary sedimentary structures and stratification sequences. SEPM Short
520 Course Notes no. 2, 161 p.
521 HARMS, J.C., SOUTHARD, J.B., and WALKER, R.G., 1982, Structures and sequences in clastic rocks.
522 SEPM Short Course Notes no. 9, 249 p.
523 HELLAND-HANSEN, W., and HAMPSON, G.J., 2009, Trajectory analysis: concepts and applications:
524 Basin Research, v. 21, p. 454-483.
525 HELLAND-HANSEN, W., STEEL, R.J., and SØMME, T.O., 2012, Shelf genesis revisited: Journal of
526 Sedimentary Research, v. 82, p. 133-148.
527 HENRIKSEN, S., HAMPSON, G.J., HELLAND-HANSEN, W., JOHANNESSEN, E.P., and STEEL, R.J., 2009,
528 Shelf edge and shoreline trajectories, a dynamic approach to stratigraphic analysis: Basin
529 Research, v. 21, p. 445-453.
530 HENRIKSEN, S., HELLAND-HANSEN, W., and BULLIMORE, S., 2011, Relationships between shelf-edge
531 trajectories and sediment dispersal along depositional dip and strike: a different approach to
532 sequence stratigraphy: Basin Research, v. 23, p. 3-21.
533 HILL, P.S., FOX, J.M., CROCKETT, J.S., CURRAN, K.J., FRIEDRICHS, C.T., GEYER, W.R., MILLIGAN, T.G.,
534 OGSTON, A.S., PUIG, P., SCULLY, M.E., TRAYKOVSKI, P.A., and WHEATCROFT, R.A., 2009,
535 Sediment Delivery to the Seabed on Continental Margins, *in* Nittrouer, C.A., Austin, J.A.,

536 Field, M.E., Kravitz, J.H., Syvitski, J.P.M., and Wiberg, P.L., eds., Continental Margin
537 Sedimentation, Blackwell Publishing Ltd., p. 49-99.
538 HODGSON, D.M., DI CELMA, C.N., BRUNT, R.L., and FLINT, S.S., 2011, Submarine slope degradation
539 and aggradation and the stratigraphic evolution of channel-levee systems: Journal of the
540 Geological Society, v. 168, p. 625-628.
541 HODGSON, D.M., FLINT, S.S., HODGETTS, D., DRINKWATER, N.J., JOHANNESSEN, E.P., and LUTHI, S.M.,
542 2006, Stratigraphic Evolution of Fine-Grained Submarine Fan Systems, Tanqua Depocenter,
543 Karoo Basin, South Africa: Journal of Sedimentary Research, v. 76, p. 20-40.
544 HUBBARD, S.M., FILDANI, A., ROMANS, B.W., COVAULT, J.A., and MCHARGUE, T.R., 2010, High-relief
545 slope clinoform development: insights from outcrop, Magallanes Basin, Chile: Journal of
546 Sedimentary Research, v. 80, p. 357-375.
547 ICHASO, A.A., and DALRYMPLE, R.W., 2009, Tide- and wave-generated fluid mud deposits in the Tilje
548 Formation (Jurassic), offshore Norway: Geology, v. 37, p. 539-542.
549 JOHANNESSEN, E.P., and STEEL, R.J., 2005, Shelf-margin clinoforms and prediction of deepwater
550 sands: Basin Research, v. 17, p. 521-550.
551 JOHNSON, M.R., VAN VUUREN, C.J., VISSER, J.N.J., COLE, D.I., WICKENS, H.D.V., CHRISTIE, A.D.M., and
552 ROBERTS, D.L., 1997, The foreland Karoo Basin, South Africa *in* Selley, R.C. (ed.) African
553 Basins. Sedimentary Basins of the World. Amsterdam, Elsevier Science, 3, p. 269-317.
554 JONES, G.E.D., HODGSON, D.M., and FLINT, S.S., 2013, Contrast in the process response of stacked
555 clinothems to the shelf-slope rollover: Geosphere, v. 9, p. 299-316.
556 JONES, G.E.D., HODGSON, D.M., and FLINT, S.S., 2015, Lateral variability in clinoform trajectory,
557 process regime, and sediment dispersal patterns beyond the shelf-edge rollover in exhumed
558 basin margin-scale clinothems: Basin Research, v. 27, p. 657-680.
559 KINEKE, G., STERNBERG, R., TROWBRIDGE, J., and GEYER, W., 1996, Fluid-mud processes on the
560 Amazon continental shelf: Continental Shelf Research, v. 16, p. 667-696.
561 KINEKE, G., WOOLFE, K., KUEHL, S., MILLIMAN, J., DELLAPENNA, T., and PURDON, R., 2000, Sediment
562 export from the Sepik River, Papua New Guinea: evidence for a divergent sediment plume:
563 Continental Shelf Research, v. 20, p. 2239-2266.
564 KUEHL, S.A., LEVY, B.M., MOORE, W.S., and ALLISON, M.A., 1997, Subaqueous delta of the Ganges-
565 Brahmaputra river system: Marine Geology, v. 144, p. 81-96.

KUEHL, S.A., NITTROUER, C.A., ALLISON, M.A., FARIA, L.E.C., DUKAT, D.A., JAEGER, J.M., PACIONI, T.D., FIGUEIREDO, A.G., and UNDERKOFFLER, E.C., 1996, Sediment deposition, accumulation, and seabed dynamics in an energetic fine-grained coastal environment: Continental Shelf Research, v. 16, p. 787-815.

LIU, J., MILLIMAN, J., and GAO, S., 2001, The Shandong mud wedge and post-glacial sediment accumulation in the Yellow Sea: Geo-Marine Letters, v. 21, p. 212-218.

LIU, J.P., XU, K.H., LI, A.C., MILLIMAN, J.D., VELOZZI, D.M., XIAO, S.B., and YANG, Z.S., 2007, Flux and fate of Yangtze River sediment delivered to the East China Sea: Geomorphology, v. 85, p. 208-224.

MACKAY, D.A., and DALRYMPLE, R.W., 2011, Dynamic mud deposition in a tidal environment: the record of fluid-mud deposition in the Cretaceous Bluesky Formation, Alberta, Canada: Journal of Sedimentary Research, v. 81, p. 901-920.

MACQUAKER, J.H., TAYLOR, K.G., and GAWTHORPE, R.L., 2007, High-resolution facies analyses of mudstones: implications for paleoenvironmental and sequence stratigraphic interpretations of offshore ancient mud-dominated successions: Journal of Sedimentary Research, v. 77, p. 324-339.

MACQUAKER, J.H.S., BENTLEY, S.J., and BOHACS, K.M., 2010, Wave-enhanced sediment-gravity flows and mud dispersal across continental shelves: Reappraising sediment transport processes operating in ancient mudstone successions: Geology, v. 38, p. 947-950.

MACQUAKER, J.H.S., and BOHACS, K.M., 2007, On the Accumulation of Mud: Science, v. 318, p. 1734-1735.

MCANALLY, W., FRIEDRICHS, C., HAMILTON, D., HAYTER, E., SHRESTHA, P., RODRIGUEZ, H., SHEREMET, A., and TEETER, A., 2007, Management of Fluid Mud in Estuaries, Bays, and Lakes. I: Present State of Understanding on Character and Behavior: Journal of Hydraulic Engineering, v. 133, p. 9-22.

MCCAVE, I.N., 1972, Transport and escape of fine-grained sediment from shelf areas, *in* Swift, D.J.P., Duane, D., and Pilkey, O., eds., Shelf Sediment Transport, Stroudsburg Pennsylvania, Dowden, Hutchinson & Ross, p. 225-248.

MCCUBBIN, D.G., 1982, Barrier-island and strand-plain facies, *in* Scholle, P.A., and Spearing, D., eds., Sandstone Depositional Environments: AAPG Memoir, 31, p. 247–279.

596 McKay, M.P., Weislogel, A.L., Fildani, A., Brunt, R.L., Hodgson, D.M., and Flint, S.S., 2015, U-PB
597 zircon tuff geochronology from the Karoo Basin, South Africa: implications of zircon recycling
598 on stratigraphic age controls: International Geology Review, v. 57, p. 393-410.
599 Mellere, D., Breda, A., and Steel, R.J., 2003, Fluvial-incised shelf-edge deltas and linkage to upper-
600 slope channels (Central Tertiary Basin, Spitsbergen): Shelf-Margin Deltas and Linked
601 Downslope Petroleum Systems: Global Significance and Future Exploration Potential, Gulf
602 Coast Section. 23rd Annual Research Conference Houston, Texas, p. 231-266.
603 Michels, K.H., Kudrass, H.R., Hübscher, C., Suckow, A., and Wiedicke, M., 1998, The submarine
604 delta of the Ganges–Brahmaputra: cyclone-dominated sedimentation patterns: Marine
605 Geology, v. 149, p. 133-154.
606 Miller, K.G., Browning, J.V., Mountain, G.S., Bassetti, M.A., Monteverde, D., Katz, M.E., Inwood,
607 J., Lofi, J., and Proust, J.-N., 2013, Sequence boundaries are impedance contrasts: Core-
608 seismic-log integration of Oligocene–Miocene sequences, New Jersey shallow shelf:
609 Geosphere, v. 9, p. 1257-1285.
610 Morton, R.A., and Suter, J.R., 1996, Sequence Stratigraphy and Composition of Late Quaternary
611 Shelf-Margin Deltas, Northern Gulf of Mexico: AAPG Bulletin, v. 80, p. 505-530.
612 Mountain, G.S., Proust, J.-N., McInroy, D., and Cotterill, C., 2010, Proceedings of the Integrated
613 Ocean Drilling Program, Volume 313: Tokyo, Integrated Ocean Drilling Program Management
614 International, Inc.
615 Mulder, T., and Alexander, J., 2001, The physical characteristics of sub-aqueous sedimentary
616 density flows and their deposits: Sedimentology, v. 48, p. 269-299.
617 Mulder, T., Syvitski, J.P.M., Migeon, S., Faugères, J.C., and Savoye B., 2003, Hyperpycnal turbidity
618 currents: initiation, behavior and related deposits: a review: Marine and Petroleum Geology
619 20, p. 861-882.
620 Muto, T., and Steel, R.J., 2002, In Defense of Shelf Edge Delta Development during Falling and
621 Lowstand of Relative Sea Level: The Journal of Geology, v. 110, p. 421-436.
622 Mutti, E., Davoli, G., Tinterri, R., and Zavala, C., 1996, The importance of fluvio-deltaic systems
623 dominated by catastrophic flooding in tectonically active basins: Memorie di Scienze
624 Geologiche, v. 48, p. 233-291.

625 MUTTI, E., TINTERRI, R., BENEVELLI, G., BIASE, D.D., and CAVANNA, G., 2003, Deltaic, mixed and
626 turbidite sedimentation of ancient foreland basins: Marine and Petroleum Geology, v. 20, p.
627 733-755.
628 NAKAJIMA, T., 2006, Hyperpycnites deposited 700 km away from river mouths in the Central Japan
629 Sea: Journal of Sedimentary Research, v. 76, p. 59-72.
630 NEMEC, W., 1995, The dynamics of deltaic suspension plumes, *in* Oti, M.N., and Postma, G., eds.,
631 Geology of Deltas, AA Balkema, Rotterdam, p. 31– 93.
632 NITTROUER, C., KUEHL, S., DEMASTER, D., and KOWSMANN, R., 1986, The deltaic nature of Amazon
633 shelf sedimentation: Geological Society of America Bulletin, v. 97, p. 444-458.
634 OGSTON, A.S., CACCHIONE, D.A., STERNBERG, R.W., and KINEKE, G.C., 2000, Observations of storm
635 and river flood-driven sediment transport on the northern California continental shelf:
636 Continental Shelf Research, v. 20, p. 2141-2162.
637 OLARIU, C., and STEEL, R.J., 2009, Influence of point-source sediment-supply on modern shelf-slope
638 morphology: implications for interpretation of ancient shelf margins: Basin Research, v. 21, p.
639 484-501.
640 OLARIU, M.I., CARVAJAL, C.R., OLARIU, C., and STEEL, R.J., 2012, Deltaic process and architectural
641 evolution during cross-shelf transits, Maastrichtian Fox Hills Formation, Washakie Basin,
642 Wyoming: AAPG Bulletin, v. 96, p. 1931-1956.
643 OLIVEIRA, C.M.M., HODGSON, D.M., and FLINT, S.S., 2011, Distribution of soft-sediment deformation
644 structures in clinoform successions of the Permian Ecca Group, Karoo Basin, South Africa:
645 Sedimentary Geology, v. 235, p. 314-330.
646 PARSONS, J.D., BUSH, J., and SYVITSKI, J.P.M., 2001, Hyperpycnal plume formation from riverine
647 outflows with small sediment concentrations: Sedimentology, v. 48, p. 465-478.
648 PATRUNO, S., HAMPSON, G.J., and JACKSON, C.A.L., 2015, Quantitative characterisation of deltaic and
649 subaqueous clinoforms: Earth-Science Reviews, v. 142, p. 79-119.
650 PATTISON, S., 2005, Isolated highstand shelf sandstone body of turbiditic origin, lower Kenilworth
651 Member, Cretaceous Western Interior, Book Cliffs, Utah: Sedimentary Geology, v. 177, p.
652 131-144.
653 PATTISON, S., 2008, Role of wave-modified underflows in the across-shelf transport of fine-grained
654 sediments: Examples from the Book Cliffs, Utah, AAPG Hedberg Conference Sediment

655 Transfer from Shelf to Deepwater - Revisiting the Delivery Mechanisms, March 3–7, 2008:
656 Ushuaia-Patagonia, Argentina.
657 PLINK-BJÖRKLUND, P., and STEEL, R., 2002, Sea-level fall below the shelf edge, without basin-floor
658 fans: Geology, v. 30, p. 115-118.
659 PLINK-BJÖRKLUND, P., and STEEL, R.J., 2004, Initiation of turbidity currents: Outcrop evidence for
660 Eocene hyperpycnal flow turbidites: Sedimentary Geology, v. 165, p. 29-52.
661 PLINT, A.G., 2014, Mud dispersal across a Cretaceous prodelta: storm-generated, wave-enhanced
662 sediment gravity flows inferred from mudstone microtexture and microfacies: Sedimentology,
663 v. 61, p. 609-647.
664 PLINT, A.G., MACQUAKER, J.H., and VARBAN, B.L., 2012, Bedload transport of mud across a wide,
665 storm-influenced ramp: Cenomanian–Turonian Kaskapau Formation, Western Canada
666 Foreland Basin: Journal of Sedimentary Research, v. 82, p. 801-822.
667 PLINT, A.G., TYAGI, A., HAY, M.J., VARBAN, B.L., ZHANG, H., and ROCA, X., 2009, Clinoforms,
668 paleobathymetry, and mud dispersal across the Western Canada Cretaceous foreland basin:
669 evidence from the Cenomanian Dunvegan Formation and contiguous strata: Journal of
670 Sedimentary Research, v. 79, p. 144-161.
671 PORĘBSKI, S.J., and STEEL, R.J., 2006, Deltas and sea-level change: Journal of Sedimentary
672 Research, v. 76, p. 390-403.
673 POSAMENTIER, H.W., JERVEY, M.T., and VAIL, P.R., 1988, Eustatic controls of clastic deposition I -
674 Conceptual framework, *in* Wilgus, C.K., Hastings, B.S., Kendall, C.G., Posamentier, H.W.,
675 Ross, C.A., and Van Wagoner, J.C., eds., Sea-Level Changes: An Integrated Approach,
676 SEPM Special Publication, 42, p. 109-124.
677 POSAMENTIER, H.W., and VAIL, P.R., 1988, Eustatic controls of clastic deposition II - Sequence and
678 systems tract model, *in* Wilgus, C.K., Hastings, B.S., Kendall, C.G., Posamentier, H.W., Ross,
679 C.A., and Van Wagoner, J.C., eds., Sea-Level Changes: An Integrated Approach, SEPM
680 Special Publication, 42, p. 109-124.
681 PYLES, D.R., and SLATT, R.M., 2007, Applications to understanding shelf edge to base-of-slope
682 changes in stratigraphic architecture of prograding basin margins: Stratigraphy of the Lewis
683 Shale, Wyoming, USA, *in* Nilsen, T.H., Shew, R.D., Steffens, G.S., and Studlick, J.R.J., eds.,
684 Atlas of Deepwater Outcrops: AAPG Studies in Geology 56, p. 485-489.

685 PYSKLYWEC, R.N., and MITROVICA, J.X., 1999, The role of subduction-induced subsidence in the
686 evolution of the Karoo Basin: Journal of Geology, v. 107, p. 155-164.
687 REINECK, H.-E., and SINGH, I.B., 1973, Depositional sedimentary environments. New York, Springer-
688 Verlag, 439 p.
689 RINE, J., and GINSBURG, R.N., 1985, Depositional facies of a mud shoreface in Suriname, South
690 America--a mud analogue to sandy, shallow-marine deposits: Journal of Sedimentary
691 Research, v. 55, p. 633-652.
692 ROSS, W.C., HALLIWELL, B.A., MAY, J.A., WATTS, D.E., and SYVITSKI, J.P.M., 1994, Slope readjustment:
693 a new model for the development of submarine fans and aprons: Geology, v. 22, p. 511-514.
694 ROTONDO, K.A., and BENTLEY, S.J., 2003, Marine dispersal of fluvial sediments as fluid muds: old
695 concept, new significance, *in* Scott, E.D., Bouma, A.H., and Bryant, W.R., eds., Siltstones,
696 Mudstones and Shales: Depositional Processes and Characteristics: SEPM, CD-ROM, p. 23-
697 34.
698 RUBIDGE, B.S., HANCOX, P.J., and CATUNEANU, O., 2000, Sequence analysis of the Ecca-Beaufort
699 contact in the southern Karoo of South Africa: South African Journal of Geology, v. 1, p. 81-
700 96.
701 RYAN, M.C., HELLAND-HANSEN, W., JOHANNESSEN, E.P., and STEEL, R.J., 2009, Erosional vs.
702 accretionary shelf margins: the influence of margin type on deepwater sedimentation: an
703 example from the Porcupine Basin, offshore western Ireland: Basin Research, v. 21, p. 676-
704 703.
705 SANCHEZ, C.M., FULTHORPE, C.S., and STEEL, R.J., 2012, Miocene shelf-edge deltas and their impact
706 on deepwater slope progradation and morphology, Northwest Shelf of Australia: Basin
707 Research, v. 24, p. 683-698.
708 SCHIEBER, J., SOUTHARD, J., and THAISEN, K., 2007, Accretion of Mudstone Beds from Migrating
709 Floccule Ripples: Science, v. 318, p. 1760-1763.
710 SCHIEBER, J., and SOUTHARD, J.B., 2009, Bedload transport of mud by floccule ripples—Direct
711 observation of ripple migration processes and their implications: Geology, v. 37, p. 483-486.
712 SCHIEBER, J., SOUTHARD, J.B., and SCHIMMELMANN, A., 2010, Lenticular shale fabrics resulting from
713 intermittent erosion of water-rich muds—interpreting the rock record in the light of recent
714 flume experiments: Journal of Sedimentary Research, v. 80, p. 119-128.

715 SCHIEBER, J., and YAWAR, Z., 2009, A new twist on mud deposition—mud ripples in experiment and
716 rock record: The Sedimentary Record, v. 7, p. 4-8.
717 SLINGERLAND, R., DRISCOLL, N.W., MILLIMAN, J.D., MILLER, S.R., and JOHNSTONE, E.A., 2008, Anatomy
718 and growth of a Holocene clinothem in the Gulf of Papua: Journal of Geophysical Research:
719 Earth Surface, v. 113, p. F01S13.
720 SOUTHARD, J.B., and STANLEY, D.J., 1976, Shelf-break processes and sedimentation, *in* Stanley, D.J.,
721 and Swift, D.J.P., eds., Marine Sediment Transport and Environmental Management. Wiley-
722 Interscience, New York, p. 351-377.
723 SOYINKA, O., and SLATT, R.M., 2008, Identification and microstratigraphy of hyperpycnites and
724 turbidites in Cretaceous Lewis Shale, Wyoming: Sedimentology, v. 55, p. 1117-1133.
725 STEEL, R., MELLERE, D., PLINK-BJÖRKLUND, P., CRABAUGH, J., DEIBERT, J., and SHELLPEPER, M., 2000,
726 Deltas vs rivers on the shelf edge: their relative contributions to the growth of shelf-margins
727 and basin-floor fans (Barremian and Eocene, Spitsbergen). *in* Weimer, P., Slatt, R.M.,
728 Coleman, J., Rosen, N.C., Nelson, H., Bouma, A.H., Styzen, M.J., and Lawrence, D.T., eds.,
729 Transactions Gulf Coast SEPM Annual Conference, Houston. CD, p. 981- 1009.
730 STEEL, R., and OLSEN, T., 2002, Clinoforms, clinoform trajectories and deepwater sands.: GCSSEPM
731 Foundation 22nd Annual Research Conference Special Publication, CD. GCSSEPM, p. 367–
732 381.
733 STEEL, R., POREBSKI, S., PLINK-BJORKLUND, P., MELLERE, D., and SCHELLPEPER, M., 2003, Shelf-edge
734 delta types and their sequence-stratigraphic relationships: Shelf-Margin Deltas and Linked
735 Downslope Petroleum Systems: Global Significance and Future Exploration Potential, Gulf
736 Coast Section. 23rd Annual Research Conference Houston, Texas, p. 205-230.
737 STEVENSON, C.J., JACKSON, C.A.-L., HODGSON, D.M., HUBBARD, S.M., and EGGENHUISEN, J.T., 2015,
738 Deep-water sediment bypass: Journal of Sedimentary Research, v. 85, p. 1058-1081.
739 TA, T.K.O., NGUYEN, V.L., TATEISHI, M., KOBAYASHI, I., and SAITO, Y., 2005, Holocene Delta Evolution
740 and Depositional Models of the Mekong River Delta, Southern Vietnam, *in* Liviu Giosan, and
741 Janok P. Bhattacharya, eds., River Deltas-Concepts, Models, and Examples. SEPM Special
742 Publication No. 83, p. 453-466.
743 TANKARD, A., WELSINK, H., AUKES, P., NEWTON, R., and STETTLER, E., 2009, Tectonic evolution of the
744 Cape and Karoo basins of South Africa: Marine and Petroleum Geology, v. 26, p. 1379-1412.

745 TAYLOR, A., GOLDRING, R., and GOWLAND, S., 2003, Analysis and application of ichnofabrics: Earth-
746 Science Reviews, v. 60, p. 227-259.
747 TRAYKOVSKI, P., GEYER, W.R., IRISH, J., and LYNCH, J., 2000, The role of wave-induced density-driven
748 fluid mud flows for cross-shelf transport on the Eel River continental shelf: Continental Shelf
749 Research, v. 20, p. 2113-2140.
750 UROZA, C.A., and STEEL, R.J., 2008, A highstand shelf-margin delta system from the Eocene of West
751 Spitsbergen, Norway: Sedimentary Geology, v. 203, p. 229-245.
752 VAIL, P.R., MITCHUM, R.M.J., TOOD, R.G., WIDMIER, J.M., THOMPSON, S., SANGREE, J.B., BUBB, J.N.,
753 and HATLELID, W.G., 1977, Seismic stratigraphy and global changes of sea level, *in* Payton,
754 C.E., ed., Seismic Stratigraphy. Application to Hydrocarbon Exploration, AAPG Memoir, 26,
755 p. 49-205.
756 VAN WAGONER, J.C., MITCHUM, R.M., CAMPION, K.M., and RAHMANIAN, V.D., 1990, Siliciclastic
757 sequence stratigraphy in well logs, cores, and outcrops. American Association of Petroleum
758 Geologists Methods in Exploration Series, No. 7: Tulsa, Oklahoma, 55 p.
759 VARBAN, B.L., and PLINT, G.A., 2008, Palaeoenvironments, palaeogeography, and physiography of a
760 large, shallow, muddy ramp: Late Cenomanian-Turonian Kaskapau Formation, Western
761 Canada foreland basin: Sedimentology, v. 55, p. 201-233.
762 VEEVERS, J.J., COLE, D.I., and COWAN, E.J., 1994, Southern Africa: Karoo Basin and Cape Fold Belt,
763 *in* Veevers, J.J., and Powell, C.M., eds., Permian-Triassic Pangean basins and foldbelts
764 along the Panthalassan Margin of Gondwanaland. Geological Society America Memoir 184,
765 p. 223-279.
766 VISSER, J.N.J., 1997, Deglaciation sequences in the Permo-Carboniferous Karoo and Kalahari basins
767 of southern Africa: a tool in the analysis of cyclic glaciomarine basin fills: Sedimentology, v.
768 44, p. 507-521.
769 VISSER, J.N.J., and PRAEKELT, H.E., 1996, Subduction, mega-shear systems and Late Palaeozoic
770 basin development in the African segment of Gondwana: Geologische Rundschau, v. 85, p.
771 632-646.
772 WALSH, J., NITTROUER, C., PALINKAS, C., OGSTON, A., STERNBERG, R., and BRUNSKILL, G., 2004,
773 Clinoform mechanics in the Gulf of Papua, New Guinea: Continental Shelf Research, v. 24, p.
774 2487-2510.

775 WICKENS, H.D.V., 1994, Basin Floor Fan Building Turbidites of the Southwestern Karoo Basin,
776 Permian Ecca Group, South Africa. [unpublished Unpubl. Ph.D. thesis thesis]: University of
777 Port Elizabeth, Port Elizabeth (South Africa), 233 p.
778 WILD, R., FLINT, S.S., and HODGSON, D.M., 2009, Stratigraphic evolution of the upper slope and shelf
779 edge in the Karoo Basin, South Africa: Basin Research, v. 21, p. 502-527.
780 WILD, R., HODGSON, D.M., and FLINT, S.S., 2005, Architecture and stratigraphic evolution of multiple,
781 vertically-stacked slope channel complexes, Tanqua depocentre, Karoo Basin, South Africa,
782 *in* Hodgson, D.M., and Flint, S.S., eds., Submarine Slope Systems: Processes and Products.
783 Geological Society of London Special Publication 244, p. 89-111.
784 WILSON, R.D., and SCHIEBER, J., 2014, Muddy Prodeltaic Hyperpycnites In the Lower Genesee Group
785 of Central New York, USA: Implications For Mud Transport In Epicontinental Seas: Journal of
786 Sedimentary Research, v. 84, p. 866-874.
787 ZAVALA, C., ARCURI, M., and BLANCO VALIENTE, L., 2012, The importance of plant remains as a
788 diagnostic criteria for the recognition of ancient hyperpycnites: Revue de Paléobiologie,
789 Genéve, v. 11, p. 457-469.
790 ZAVALA, C., ARCURI, M., GAMERO, H., and CONTRERAS, C., 2007, The composite bed: A new distinctive
791 feature of Hyperpycnal deposition., Annual AAPG Convention, April 2–5, 2007: Long Beach,
792 California.
793 ZAVALA, C., GAMERO, H., and ARCURI, M., 2006a, Lofting rhythmites: A diagnostic feature for the
794 recognition of hyperpycnal deposits, Topical session T136: River Generated Hyperpycnal
795 Events and Resulted Deposits in Modern and Ancient Environments. 2006 GSA Annual
796 Meeting, 22-25 October: Philadelphia, PA., USA.
797 ZAVALA, C., PONCE, J., ARCURI, M., DRITTANTI, D., FREIJE, H., and ASENSIO, M., 2006b, Ancient
798 Lacustrine hyperpycnites: a depositional model from a case study in the Rayoso Formation
799 (Cretaceous) of west-central Argentina: Journal of Sedimentary Research, v. 76, p. 40-58.
800
801
802

List of figures

Figure 1: Cartoon showing nomenclature and main characteristics of shelf-edge versus shelf-confined clinothems. Based on Johannessen and Steel (2005); Helland-Hansen and Hampson (2009); Mountain et al. (2010); Jones et al. (2013).

Figure 2: Map and general stratigraphy of the SW Karoo Basin showing the Waterford Formation outcrop belt and the location of sedimentary logs and correlation panels in the Tanqua and Laingsburg depocenters. Note that the stratigraphic intervals studied in the two depocenters are not correlated. Stratigraphy modified from Flint et al. (2011).

Figure 3: Correlation panel of the basin margin succession in the Tanqua depocenter, showing the clinoform stacking of the lower Waterford Formation. Correlation displays thirteen parasequences (C1-13), with their flooding surfaces and main sequence stratigraphic boundaries, as well as the interpreted position of shelf edge rollovers, based on major gradient changes combined with secondary criteria including outcrop-scale growth faults, widespread erosion (gullies) and increase in sandstone turbidites beyond the shelf edge (Jones et al. 2013). A regional mudstone unit on top of Unit 5 acts as a correlation datum. Modified from Wild et al. (2009).

Figure 4: Correlation panel of the lower Waterford Formation in the Laingsburg depocenter. The Baviaans South (BS), Baviaans North (BN) and Zoutkloof (Z) correlation panels encompass eight lower Waterford parasequences (WfC 1-8). Sequence boundaries, flooding surfaces and a type 2 sequence boundary between WfC 5 and WfC 6 are shown. The panels use top of Unit F as a correlation datum. Modified from Jones et al. (2015). Same color code as in Figure 3.

Figure 5: Paleogeographic map reconstructions of WfC 6 (A) and WfC 7 (B) from the data shown in the correlation panels of Fig. 4. (C) Map view of the evolution of the shelf-edge rollover position through time in the Laingsburg depocenter. Note that during WfC 6 and WfC 7 the position of the sand pinchout is not coincident with the interpreted location of the shelf edge rollover.

Figure 6: Representative sedimentary log from the Faberskraal farm locality (Z10, see location in Figure 4A), showing a lower fining-upward unit with bioturbated and nodular siltstones included in the TST associated with WfC 5, followed by an overall coarsening and thickening-up succession (WfC 6-7) of non- to moderately-bioturbated shoreface-offshore transition (SOT) thin beds passing into thicker lower shoreface deposits. Same color code used in Figure 3.

Figure 7: Detailed view of the correlation along the Zoutkloof area, showing progradation during WfC 6-7 after the regional transgression above WfC 5. The absence of delta front/shoreface deposits beyond the WfC 5 shelf-edge rollover position in WfC 6-7 suggests their sand-rich components are shelf-confined deltas (as their sand pinch-out position indicates), with mud-dominated shelf-edge rollovers. Note the low net progradation of the shelf-edge between WfC 4-5 compared with the basinward shift of the sand-rich deformed facies of WfC 8 over 50 m of mudstones of WfC 6-7 and about 15 km beyond the pre-established sand-dominated shelf-edge rollover of WfC 5.

Figure 8: General stratigraphic section of the SL1 research borehole, in the Tanqua depocenter, with detailed sketches/photographs of key mudstone beds (1-6) along C6 and C7. Note the vertical scale of the logs is in centimeters. Cycles in the well log are based on the recognition of flooding surfaces in the core (Wild et al. 2009). VSH = Shale volume from Gamma Ray log.

Figure 9: Enlarged view of a polished outcrop sample of a typical bi-partite (*Type B*) thin bed. Note the internal complexity of mud-rich thin beds and the difficulty to recognize their subdivisions in outcrop due to their small-scale expression.

Figure 10: Cartoon showing the interpreted spatial distribution of dilute gravity flow processes and deposits across a fine-grained shelf-edge rollover associated with storm-dominated shelves. The position of the defined bed types along the depositional profile is extrapolated from their stratigraphic distribution.

Figure 11: Sketch of shelf-edge rollover areas based in the Waterford Formation stacked basin margin clinothems, with temporal flooded shelf conditions, showing the complexity in rollover

identification and potential risks of clinoform trajectory analysis based on identification of sand-rich rollovers.

Tables

Table 1. Summary of sedimentary facies and facies associations found from the shelf to upper slope of the lower Waterford Fm. based on previous works (Wild et al. 2009; Oliveira et al. 2011; Jones et al. 2013; 2015)

Table 2. Clinoform thickness and slope variability in the Tanqua and Laingsburg depocenters. Estimated gradients and trajectories are from compacted thickness measurements (see also Wild et al. 2009).

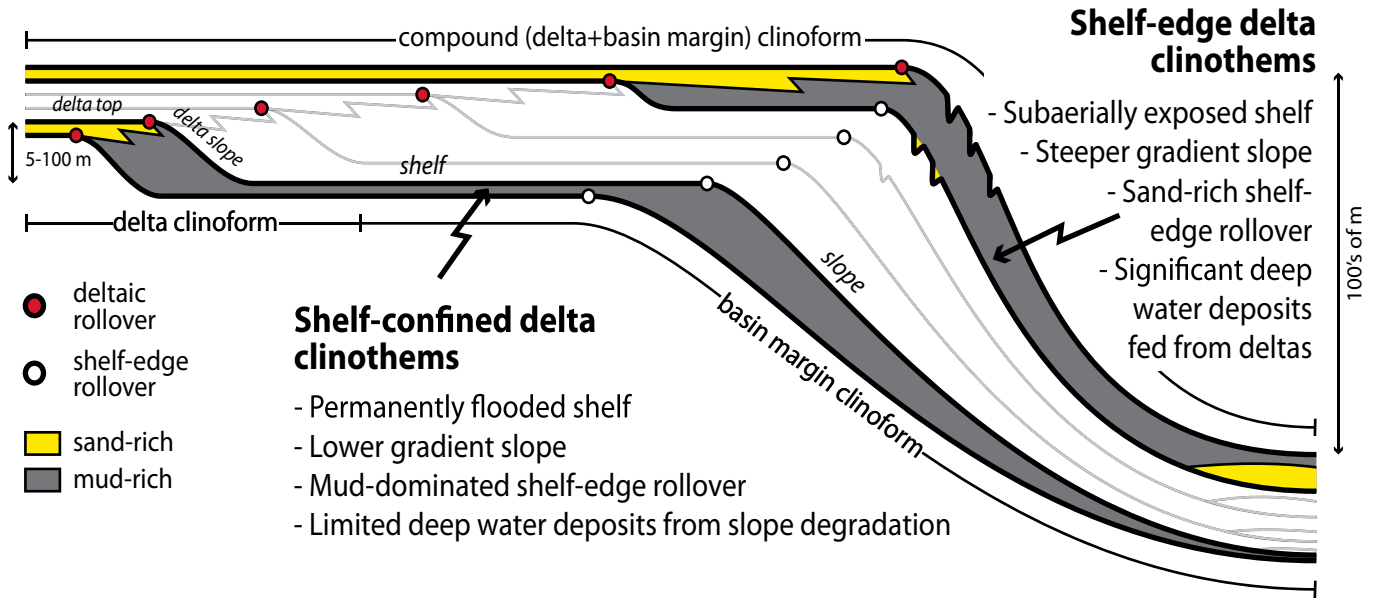
compound (delta+basin margin) clinoform
delta top
delta slope
5-100 m
shelf
delta clinoform
slope
basin margin clinoform
deltaic rollover
shelf-edge rollover
sand-rich
mud-rich
Shelf-confined delta clinothems
- Permanently flooded shelf
- Lower gradient slope
- Mud-dominated shelf-edge rollover
- Limited deep water deposits from slope degradation
Shelf-edge delta clinothems
- Subaerially exposed shelf
- Steeper gradient slope
- Sand-rich shelf-edge rollover
- Significant deep water deposits fed from deltas
100's of m

Fig. 1

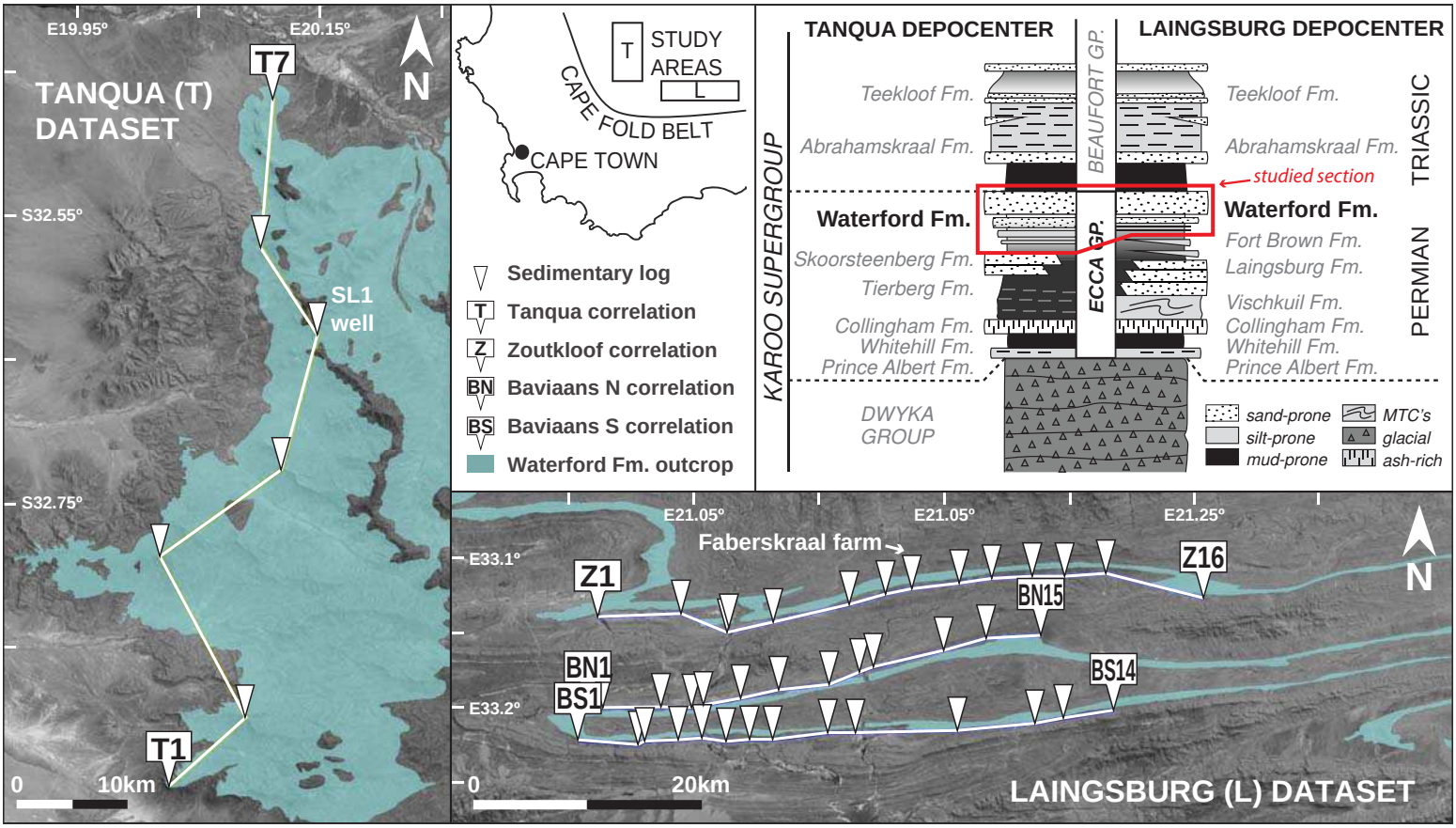
E19.95°
E20.15°
TANQUA (T) DATASET
T7
N
S32.55°
SL1 well
S32.75°
T1
0
10km
STUDY AREAS
T
L
CAPE FOLD BELT
CAPE TOWN
Sedimentary log
Tanqua correlation
Zoutkloof correlation
Baviaans N correlation
Baviaans S correlation
Waterford Fm. outcrop
TANQUA DEPOCENTER
LAINGSBURG DEPOCENTER
KAROO SUPERGROUP
BEAUFORT GP.
ECCA GP.
Teekloof Fm.
Abrahamskraal Fm.
studied section
Waterford Fm.
Skoorsteenberg Fm.
Tierberg Fm.
Collingham Fm.
Whitehill Fm.
Prince Albert Fm.
Fort Brown Fm.
Laingsburg Fm.
Vischkuil Fm.
DWYKA GROUP
TRIASSIC
PERMIAN
sand-prone
silt-prone
mud-prone
MTC's
glacial
ash-rich
E21.05°
E21.05°
E21.25°
Faberskraal farm
E33.1°
E33.2°
Z1
Z16
BN15
BN1
BS1
BS14
N
0
20km
LAINGSBURG (L) DATASET

Fig. 2

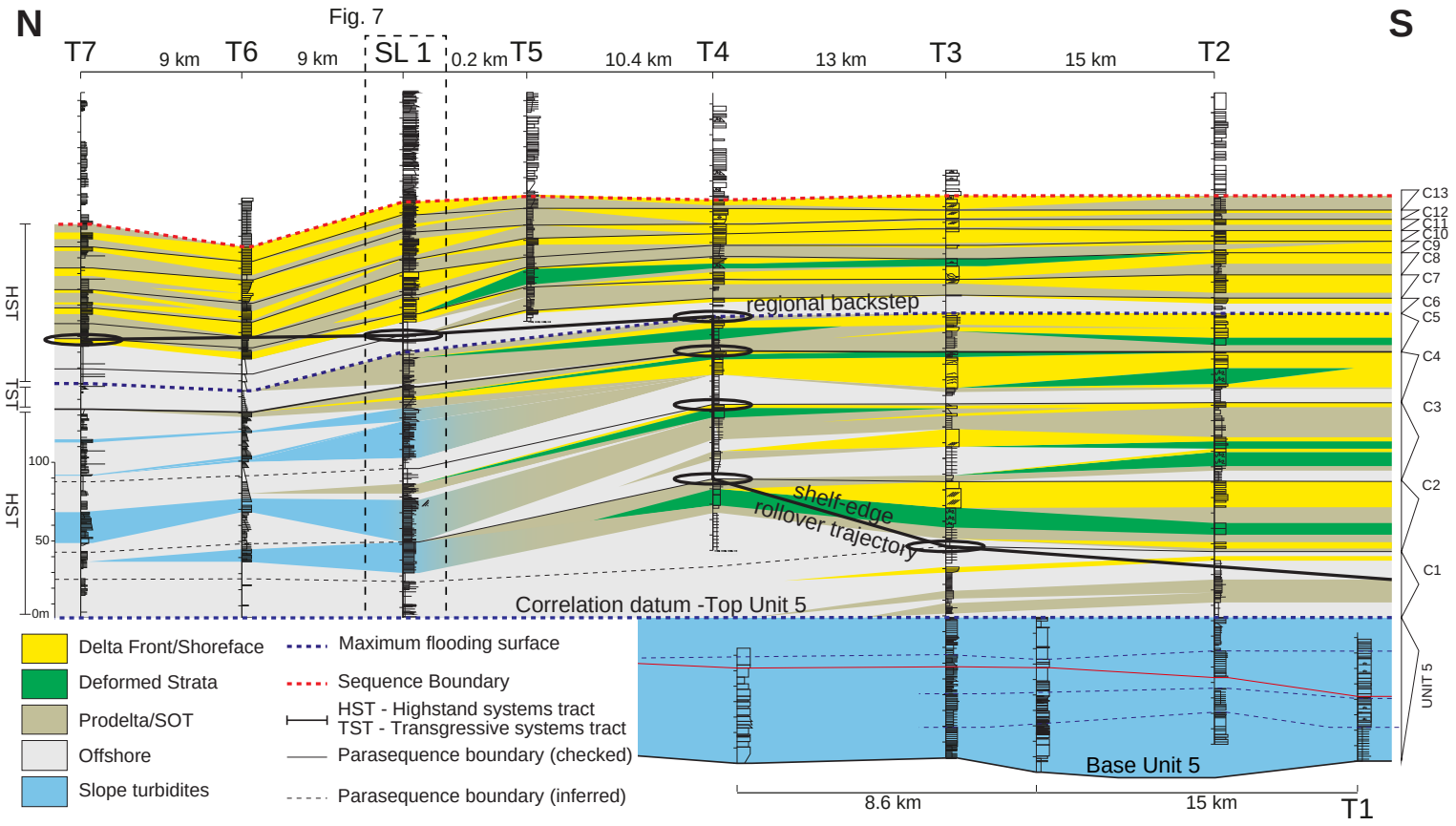
N
Fig. 7
S
T7
9 km
T6
9 km
SL 1
0.2 km
T5
10.4 km
T4
13 km
T3
15 km
T2
HST
TST
HST
100
50
0m
regional backstep
shelf-edge
rollover trajectory
Correlation datum -Top Unit 5
C13
C12
C11
C10
C9
C8
C7
C6
C5
C4
C3
C2
C1
UNIT 5
Base Unit 5
8.6 km
15 km
T1
Delta Front/Shoreface
Deformed Strata
Prodelta/SOT
Offshore
Slope turbidites
Maximum flooding surface
Sequence Boundary
HST - Highstand systems tract
TST - Transgressive systems tract
Parasequence boundary (checked)
Parasequence boundary (inferred)

Fig. 3

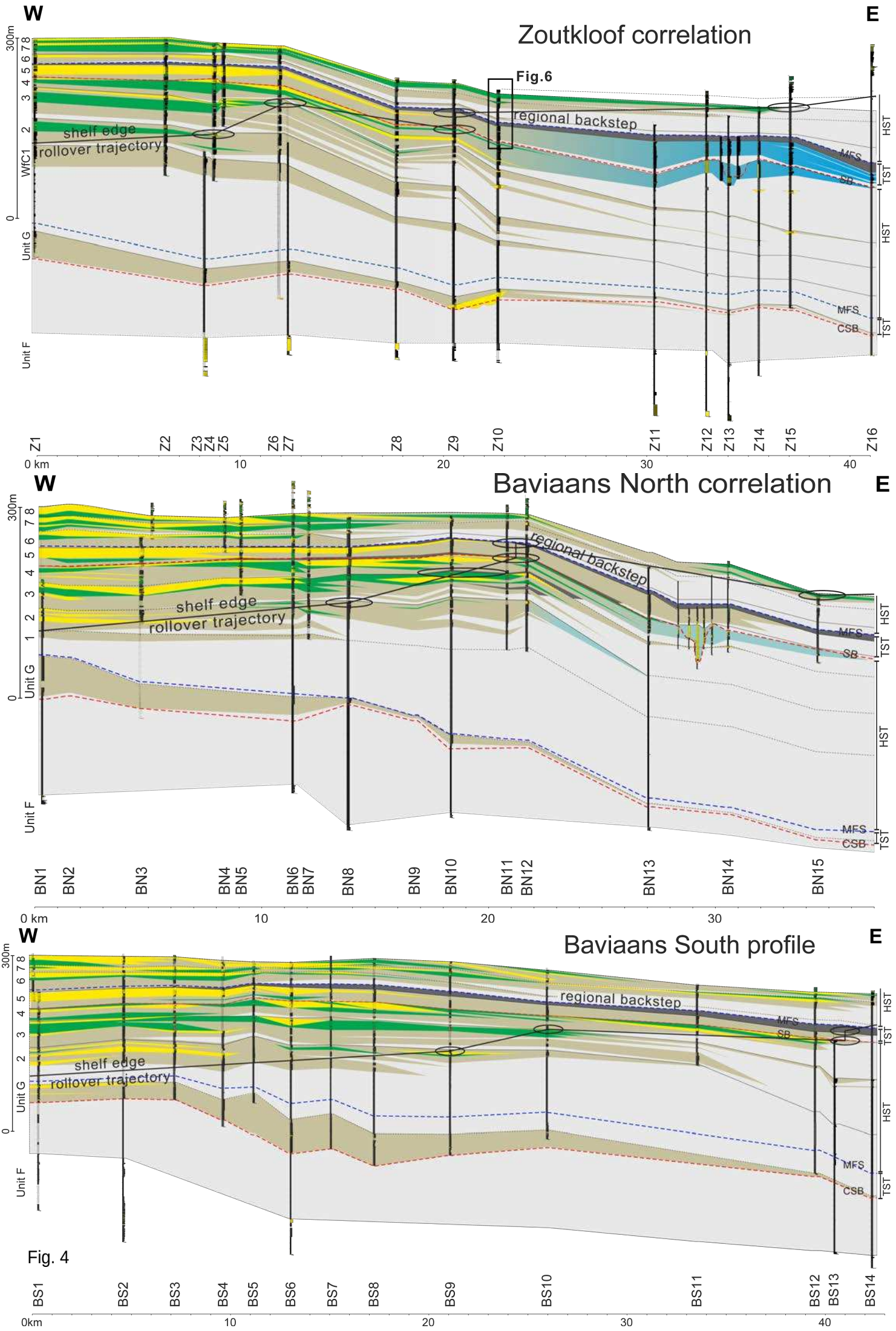
W
E
Zoutkloof correlation
Fig.6
regional backstep
shelf edge
rollover trajectory
MFS
SB
MFS
CSB
HST
TST
HST
TST
300m
0
WfC1
Unit G
Unit F
Z1
Z2
Z3
Z4
Z5
Z6
Z7
Z8
Z9
Z10
Z11
Z12
Z13
Z14
Z15
Z16
0 km
10
20
30
40
W
E
Baviaans North correlation
regional backstep
shelf edge
rollover trajectory
MFS
SB
MFS
CSB
HST
TST
HST
TST
300m
0
Unit G
Unit F
BN1
BN2
BN3
BN4
BN5
BN6
BN7
BN8
BN9
BN10
BN11
BN12
BN13
BN14
BN15
0 km
10
20
30
W
E
Baviaans South profile
regional backstep
shelf edge
rollover trajectory
MFS
SB
MFS
CSB
HST
TST
HST
TST
300m
0
Unit G
Unit F
BS1
BS2
BS3
BS4
BS5
BS6
BS7
BS8
BS9
BS10
BS11
BS12
BS13
BS14
0km
10
20
30
40

Fig. 4

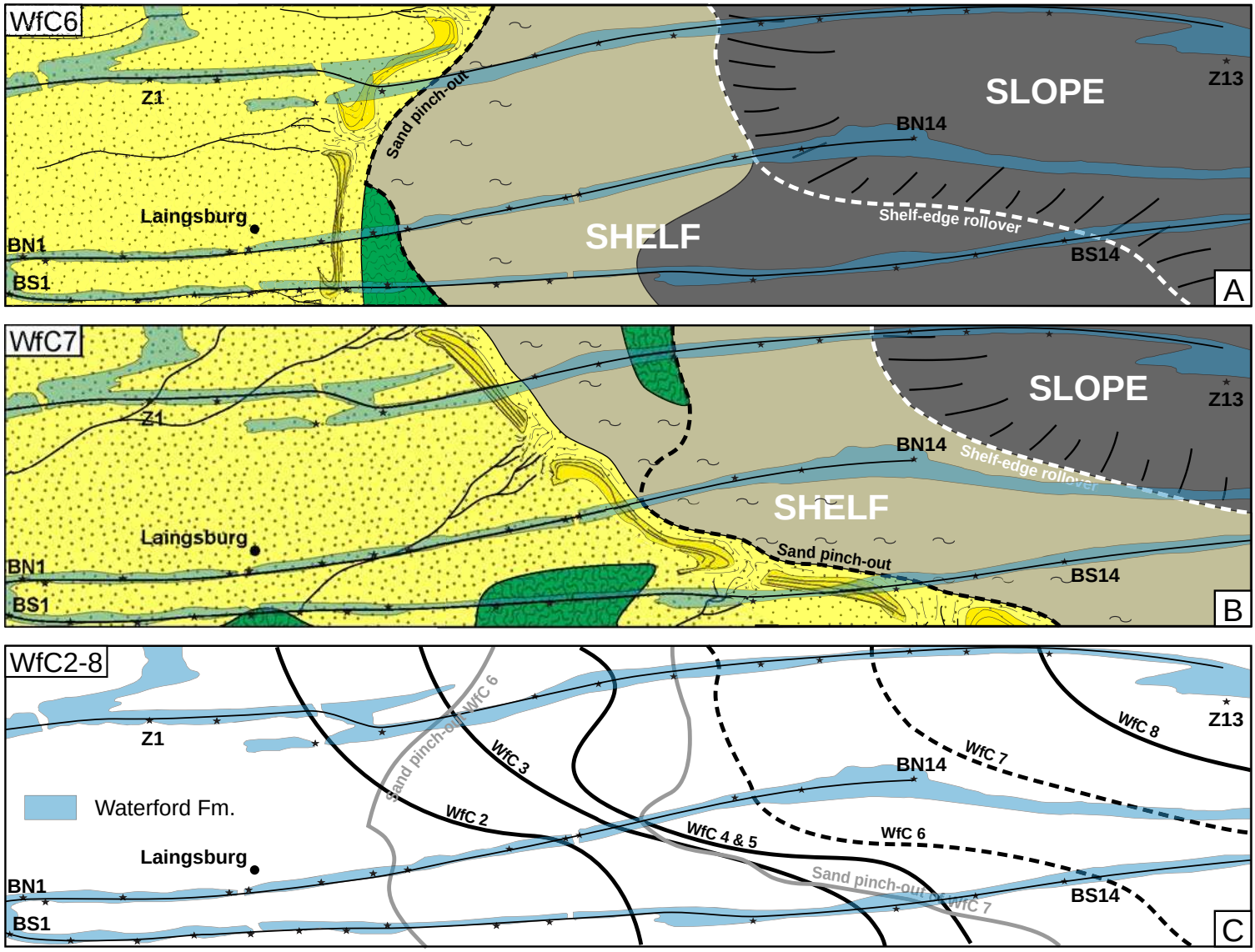
WfC6
Z1
Sand pinch-out
SLOPE
Z13
BN14
Laingsburg
SHELF
Shelf-edge rollover
BN1
BS1
BS14
A
WfC7
Z1
SLOPE
Z13
BN14
Shelf-edge rollover
SHELF
Laingsburg
Sand pinch-out
BN1
BS1
BS14
B
WfC2-8
Z1
Sand pinch-out WfC 6
WfC 3
WfC 8
Z13
WfC 7
BN14
Waterford Fm.
WfC 2
WfC 4 & 5
WfC 6
Laingsburg
Sand pinch-out WfC 7
BN1
BS14
BS1
C
0
10km
Delta front/shoreface sandstones
Correlated sedimentary logs
Deformed sandstones
Prodelta/SOT transition thin beds
Offshore/slope mudstones
Sand pinch-out
Sandy shelf-edge rollover
Muddy shelf edge rollover

Fig. 5

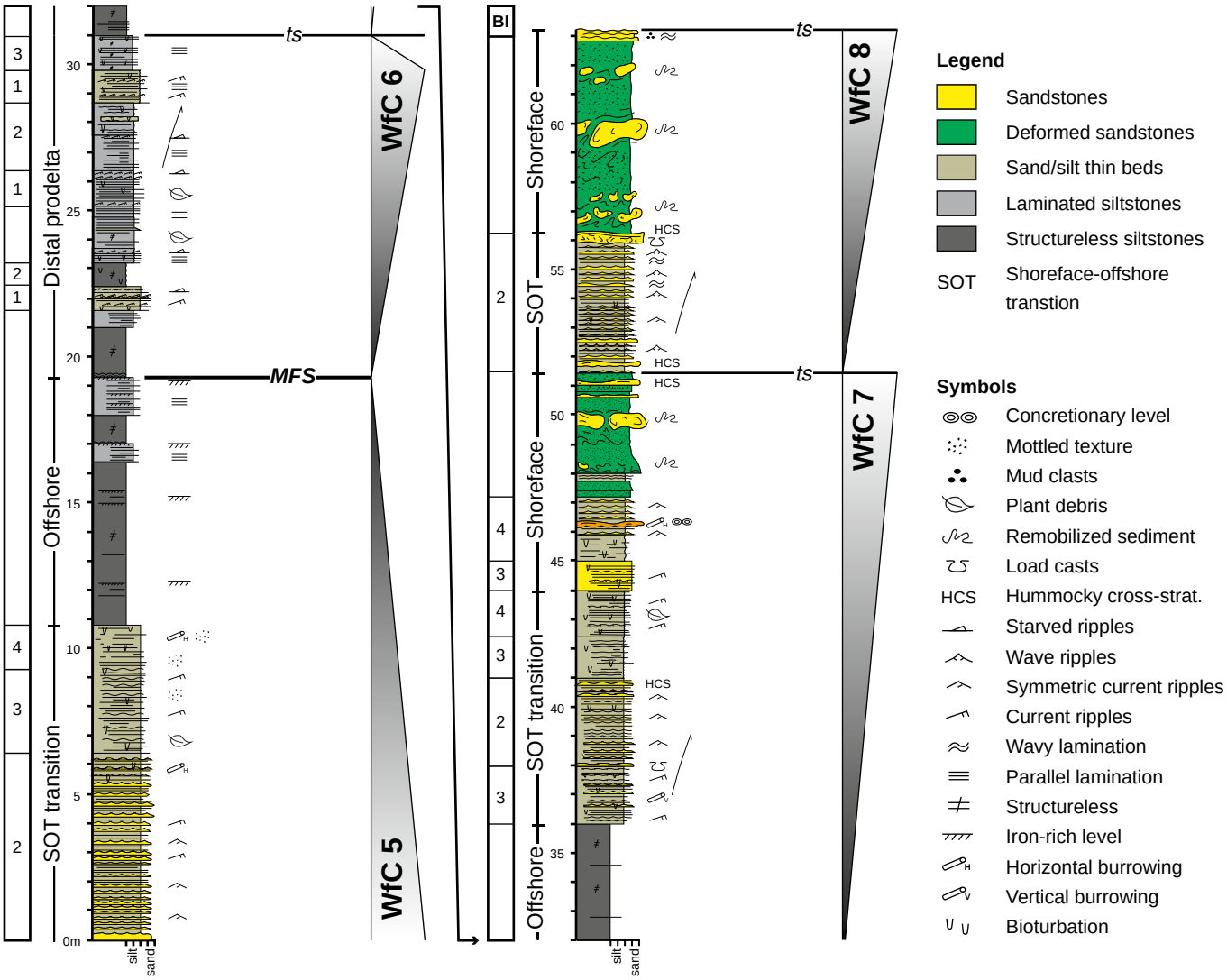
Distal prodelta
Offshore
SOT transition
Shoreface
SOT
Shoreface
SOT transition
Offshore
ts
MFS
ts
ts
WfC 6
WfC 5
WfC 8
WfC 7
HCS
HCS
HCS
HCS
BI
0m
5
10
15
20
25
30
35
40
45
50
55
60
silt
sand
silt
sand
Legend
Sandstones
Deformed sandstones
Sand/silt thin beds
Laminated siltstones
Structureless siltstones
SOT
Shoreface-offshore transtion
Symbols
Concretionary level
Mottled texture
Mud clasts
Plant debris
Remobilized sediment
Load casts
HCS
Hummocky cross-strat.
Starved ripples
Wave ripples
Symmetric current ripples
Current ripples
Wavy lamination
Parallel lamination
Structureless
Iron-rich level
Horizontal burrowing
Vertical burrowing
Bioturbation

Fig. 6

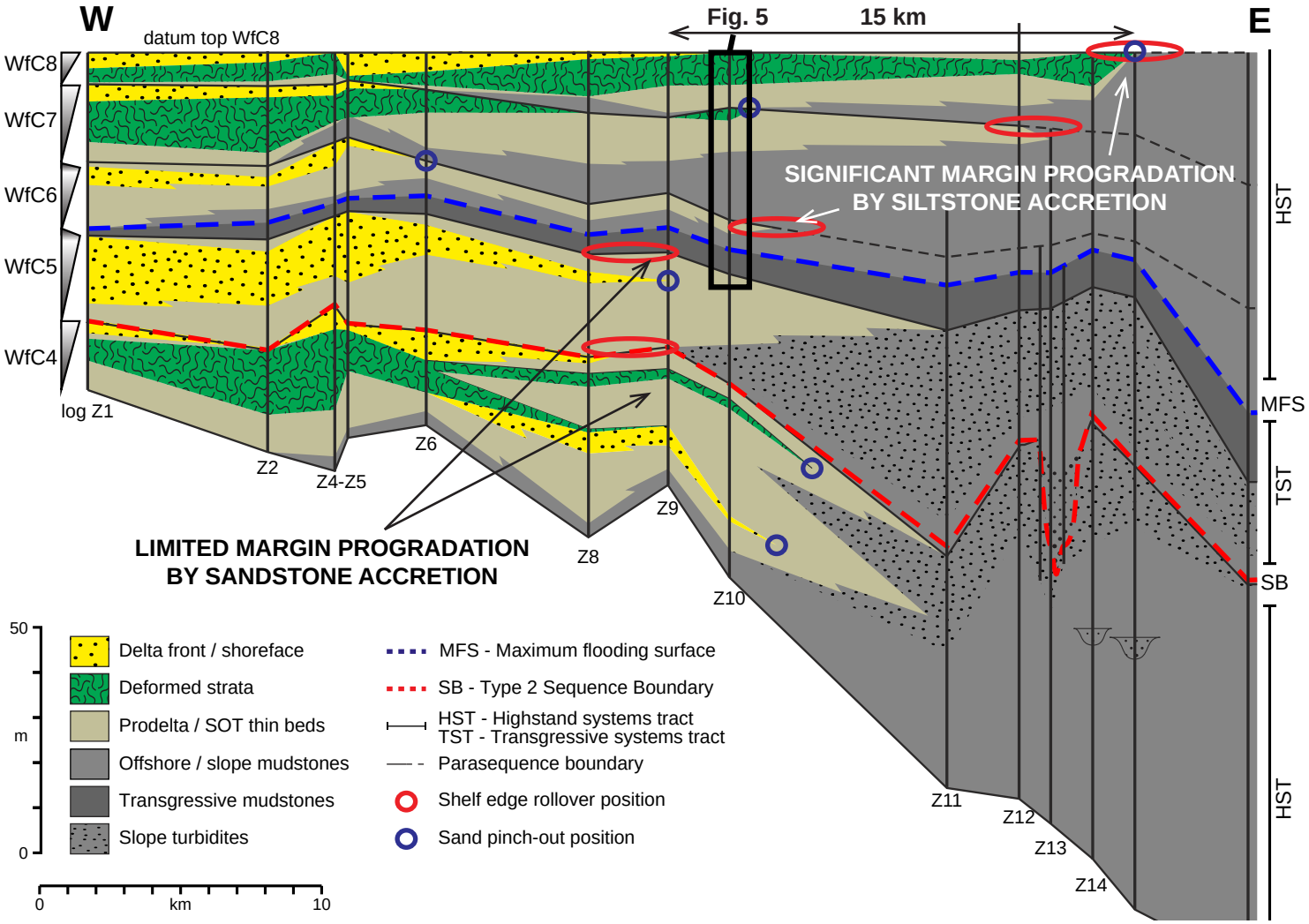
W
E
datum top WfC8
Fig. 5
15 km
WfC8
WfC7
WfC6
WfC5
WfC4
log Z1
Z2
Z4-Z5
Z6
Z8
Z9
Z10
Z11
Z12
Z13
Z14
SIGNIFICANT MARGIN PROGRADATION
BY SILTSTONE ACCRETION
LIMITED MARGIN PROGRADATION
BY SANDSTONE ACCRETION
HST
MFS
TST
SB
HST
50
m
0
0
km
10
Delta front / shoreface
Deformed strata
Prodelta / SOT thin beds
Offshore / slope mudstones
Transgressive mudstones
Slope turbidites
MFS - Maximum flooding surface
SB - Type 2 Sequence Boundary
HST - Highstand systems tract
TST - Transgressive systems tract
Parasequence boundary
Shelf edge rollover position
Sand pinch-out position

Fig. 7

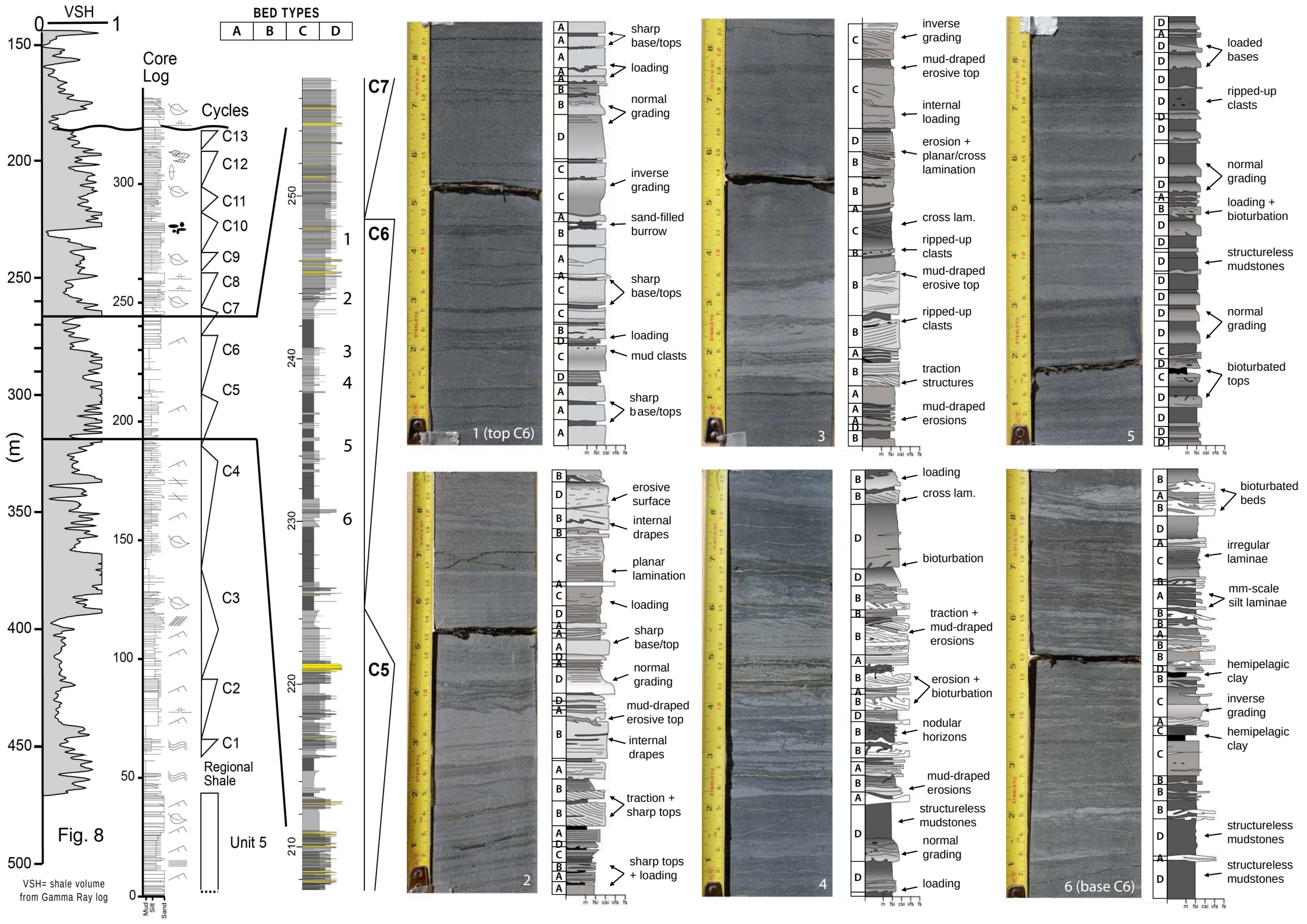
VSH
0
1
BED TYPES
A
B
C
D
Core Log
Cycles
C13
C12
C11
C10
C9
C8
C7
C6
C5
C4
C3
C2
C1
Regional Shale
Unit 5
(m)
150
200
250
300
350
400
450
500
300
250
200
150
100
50
0
250
240
230
220
210
1
2
3
4
5
6
C7
C6
C5
Mud
Silt
Sand
Fig. 8
VSH= shale volume from Gamma Ray log
sharp base/tops
loading
normal grading
inverse grading
sand-filled burrow
sharp base/tops
loading
mud clasts
sharp base/tops
1 (top C6)
inverse grading
mud-draped erosive top
internal loading
erosion + planar/cross lamination
cross lam.
ripped-up clasts
mud-draped erosive top
ripped-up clasts
traction structures
mud-draped erosions
3
loaded bases
ripped-up clasts
normal grading
loading + bioturbation
structureless mudstones
normal grading
bioturbated tops
5
erosive surface
internal drapes
planar lamination
loading
sharp base/top
normal grading
mud-draped erosive top
internal drapes
traction + sharp tops
sharp tops + loading
2
loading
cross lam.
bioturbation
traction + mud-draped erosions
erosion + bioturbation
nodular horizons
mud-draped erosions
structureless mudstones
normal grading
loading
4
bioturbated beds
irregular laminae
mm-scale silt laminae
hemipelagic clay
inverse grading
hemipelagic clay
structureless mudstones
structureless mudstones
6 (base C6)

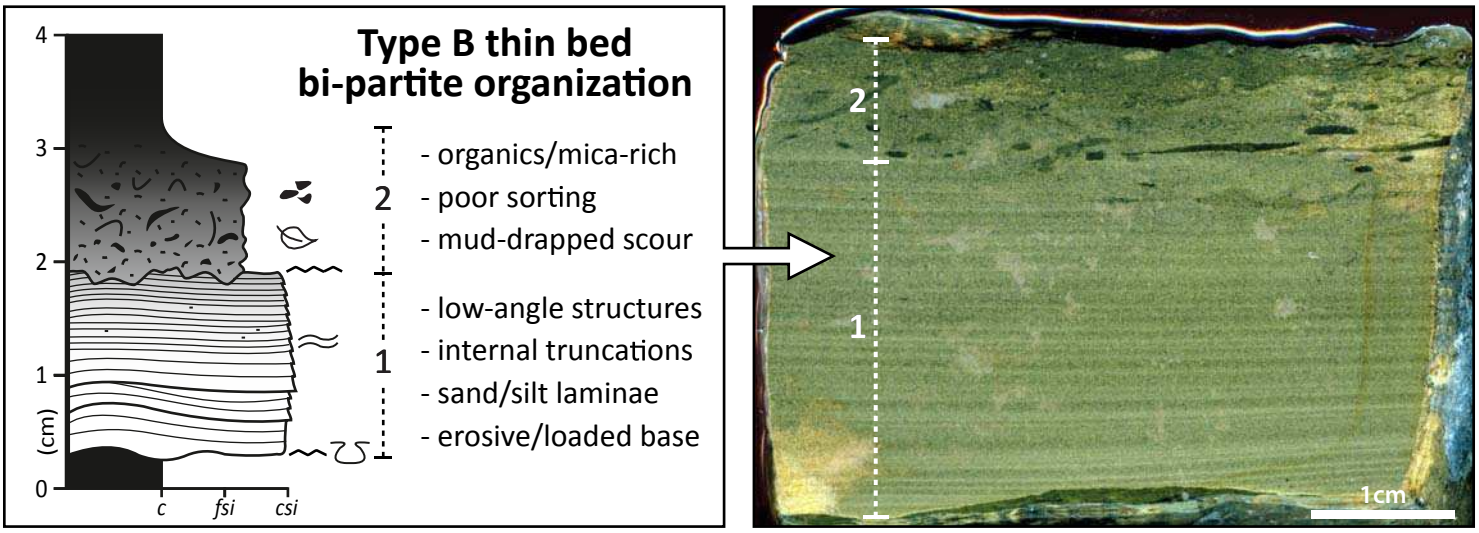
Type B thin bed
bi-partite organization
- organics/mica-rich
- poor sorting
- mud-drapped scour
- low-angle structures
- internal truncations
- sand/silt laminae
- erosive/loaded base
2
1
4
3
2
1
0
(cm)
c
fsi
csi
2
1
1cm

Fig. 9

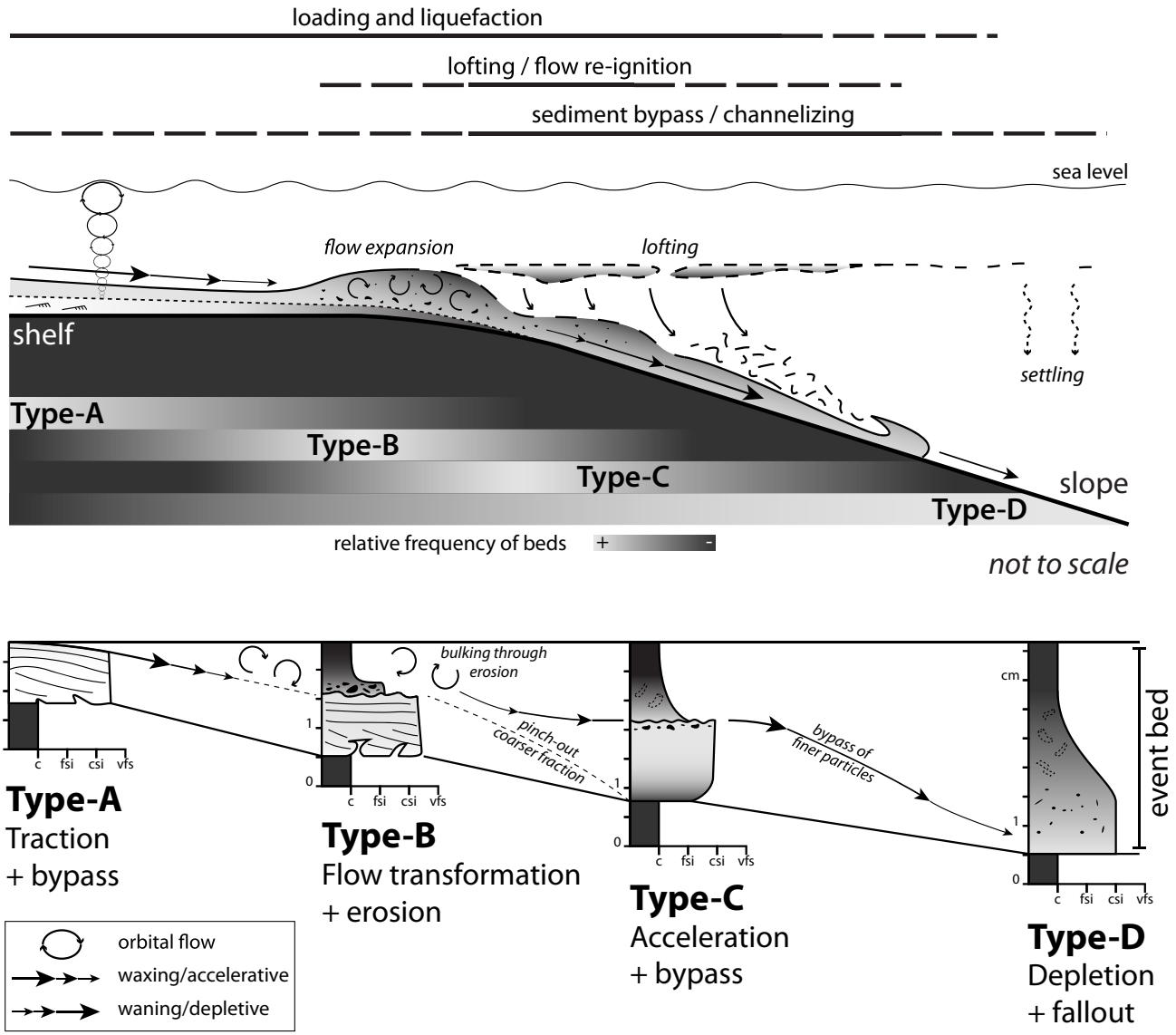
loading and liquefaction
lofting / flow re-ignition
sediment bypass / channelizing
sea level
flow expansion
lofting
settling
shelf
Type-A
Type-B
Type-C
Type-D
slope
relative frequency of beds
+
-
not to scale
bulking through erosion
pinch-out coarser fraction
bypass of finer particles
cm
event bed
c fsi csi vfs
Type-A
Traction
+ bypass
Type-B
Flow transformation
+ erosion
Type-C
Acceleration
+ bypass
Type-D
Depletion
+ fallout
orbital flow
waxing/accelerative
waning/depletive

Fig. 10

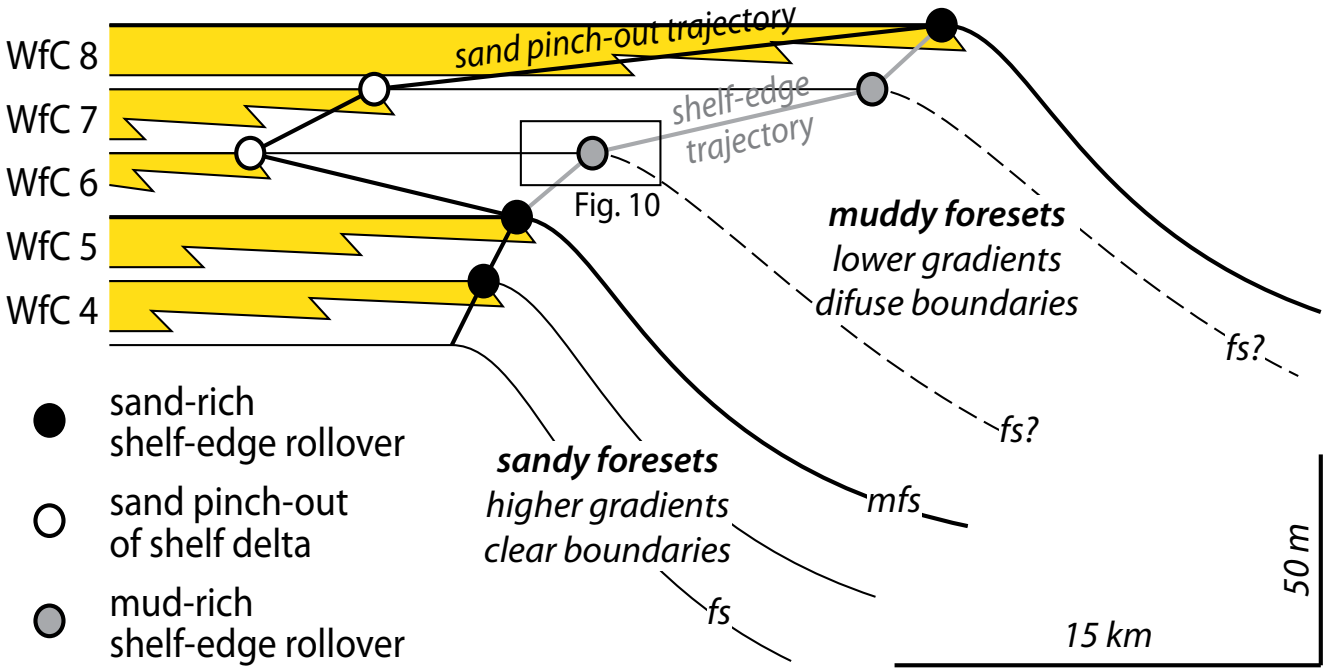
WfC 8
WfC 7
WfC 6
WfC 5
WfC 4
sand pinch-out trajectory
shelf-edge trajectory
Fig. 10
muddy foresets
lower gradients
difuse boundaries
fs?
fs?
sandy foresets
higher gradients
clear boundaries
mfs
fs
sand-rich shelf-edge rollover
sand pinch-out of shelf delta
mud-rich shelf-edge rollover
50 m
15 km

Fig. 11

Lithofacies	Structures	Contacts	Thickness	Geometry	Trace fossils and other features	Depositional process	Common facies association
Concretionary horizons	Isolated or layered nodules and concretions.	Sharp	Up to 50 cm	Lenticular to irregular	Sideritic and pre-compactional	Diagenetic processes at times of maximum sediment starvation	**Offshore**
Grey silty claystones	Structureless. Rare parallel lamination	Gradational	2 cm to m+ packages	Laterally extensive sheets	Rare. Common with concretionary horizons	Hemi-pelagic suspension settling	**Offshore**
Interbedded claystones and siltstones	Structurelss to parallel lam., starved-ripples. Normally and inversely-graded	Sharp base and gradational top	Laminae 0.1 to 1 cm. units 10 cm to 4 m	Laminae tabular to lenticular. Units often sheet like	Rare to moderate. *Chondrites, Gordia sp.*	Low concentration turbidity current, hyperpycnal or wave-enhanced gravity flow	**Offshore / prodelta**
Interbedded siltstones and sandstones	Current,wave-ripples, convex-up and parallel lam. and structureless. Normally and inversely-graded. Dewatering	Sharp base, tops gradational to sharp	1 to 5 cm	Individual beds tabular at the outcrop scale. Units display a sheet geometry	Common. *Chondrites, Helminthopsis, Helminthoida, Gordia sp. Lorenzinia, Lophoterium, Cosmorhaphe, Palaeodyctyon*	Alternation of high/low energy currents, or wave-influenced low concentration currents	**Prodelta / Shoreface-Offshore transition (SOT)**
Thin to medium bedded sandstones	Current,wave-ripples, parallel lam., structureless. Local sigmoid geometry and pinch and swell	Sharp bases to sands. Sharp to gradational tops.	Bedding of 5-10 cm, 10-20 cm and 20 cm+	Beds tabular. Sheet geometry to units	Moderate to high bioturbation indexes, particularly when observed at the top of parasequences	Low concentration turbidity current to high concentration turbidite currents, locally wave-influenced	**Lower shoreface / delta front**
Medium to thick bedded vf sandstones	Structureless, parallel lam., climbing ripples, locally sigmoidal. Some scour and fill	Bases sharp. Rarely erosional. Sharp to gradational tops	20 to 60 cm	Tabular to locally lenticular. Units form sheets and channels	Rare. *Helmenthoides, Undicna bina* (fish traces)	High concentration turbidite currents.Dominated by depletive steady flow	**Slope turbidites**
Medium to thick bedded vf-f sandstones	HCS/SCS / low angle cross-stratification. Symmetric rippled tops, dewatering	Sharp	20 cm-1 m+	Sheets	-	Traction-load deposition reworked by combined flows or waves	**Upper shoreface**
Thick-bedded vf-f sandstones (sheet-like)	Structureless, local parallel lamination. Local scour and fill. Dewatering	Sharp to erosive base. Sharp tops	50-100 cm. m+ packages due to amalgamation	Sheets	Wood fragments	Unconfined high concentration turbidite currents	**Slope turbidites (lobes)**
Thick-bedded vf-f sandstones (channel-like)	Massive local parallel lamination. Local scour and fill. Dewatering	Sharp to erosive base. Sharp tops	80cm-m+ due to amalgamation	Channel fills and some sheets	Wood fragments, rip-up clasts to the base	Confined high concentration turbidite currents with depletive-steady/non steady flows	**Slope turbidites (gullies)**
Intraclast rich conglomerates	Chaotic	Sharp and sometimes erosive	1 cm to 0.5 m	Lenticular up to 20m wide	Wood and organic debris	Debris flows, sediment bypass and localised deposition of rip up clasts	**Slope turbidites**

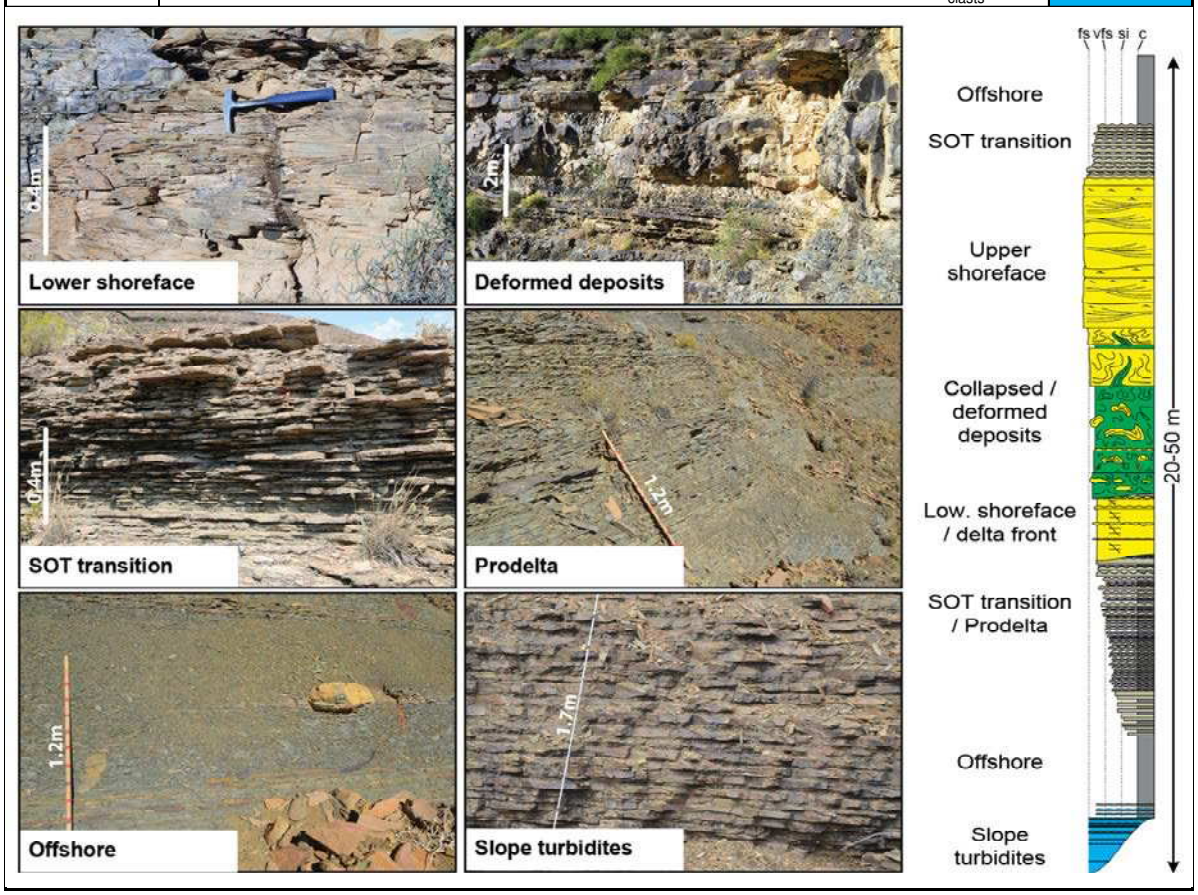

Table 1

LAINGSBURG CLINOFORMS						
Cycle	**Thickness (m)** Max	Min	**Gradient (deg)** Min (30 km)	**Slope deposits**	**Rollover trajectory**	**Dominant process**
WfC1	163.4	23.6	0.712	muddy	flat	river
WfC2	145.5	31.2	0.713	sandy	flat-rising	wave
WfC3	92	34	0.700	mud>sand	flat-rising	river/wave
WfC4	124	16.4	0.570	sandy	rising	wave
WfC5	58	10	0.531	sandy	rising	wave
WfC6	37	6.8	0.552	muddy	flat-falling	river
WfC7	38	7	0.531	muddy	flat-falling	river
WfC8	23	6.04	0.513	sandy?	falling	river

TANQUA CLINOFORMS						
Cycle	**Thickness (m)** Max	Min	**Gradient (deg)** Min (30 km)	**Slope deposits**	**Rollover trajectory**	**Dominant process**
C1	45	21	0.435	muddy	flat	river
C2	52	17	0.512	sandy	flat-rising	river/wave
C3	44	31	0.504	sand>mud	rising	river/wave
C4	54	32	0.439	mud>sand	rising	river
C5	32	13	0.455	mud>sand	rising	river/tide
C6	15	10	0.455	muddy	flat-falling	river
C7	19	9.5	0.458	muddy	flat-falling	river
C8	14	7	0.474	sand>mud	flat-rising	river

Table 2